Cell

RIG-I Detects Viral Genomic RNA during Negative-Strand RNA Virus Infection

Jan Rehwinkel,[1,5] Choon Ping Tan,[1,2,5] Delphine Goubau,[1] Oliver Schulz,[1] Andreas Pichlmair,[1,4] Katja Bier,[2] Nicole Robb,[2] Frank Vreede,[2] Wendy Barclay,[3] Ervin Fodor,[2] and Caetano Reis e Sousa[1,*]

[1]Immunobiology Laboratory, Cancer Research UK London Research Institute, 44 Lincoln's Inn Fields, London WC2A 3PX, UK
[2]Sir William Dunn School of Pathology, University of Oxford, South Parks Road, Oxford OX1 3RE, UK
[3]Department of Virology, Imperial College, St. Mary's Campus, Norfolk Place, London W2 1PG, UK
[4]Present address: Research Center for Molecular Medicine of the Austrian Academy of Sciences (CeMM), Lazarettgasse 19/3, A-1090 Vienna, Austria
[5]These authors contributed equally to this work
*Correspondence: caetano@cancer.org.uk
DOI 10.1016/j.cell.2010.01.020

SUMMARY

RIG-I is a key mediator of antiviral immunity, able to couple detection of infection by RNA viruses to the induction of interferons. Natural RIG-I stimulatory RNAs have variously been proposed to correspond to virus genomes, virus replication intermediates, viral transcripts, or self-RNA cleaved by RNase L. However, the relative contribution of each of these RNA species to RIG-I activation and interferon induction in virus-infected cells is not known. Here, we use three approaches to identify physiological RIG-I agonists in cells infected with influenza A virus or Sendai virus. We show that RIG-I agonists are exclusively generated by the process of virus replication and correspond to full-length virus genomes. Therefore, nongenomic viral transcripts, short replication intermediates, and cleaved self-RNA do not contribute substantially to interferon induction in cells infected with these negative strand RNA viruses. Rather, single-stranded RNA viral genomes bearing 5′-triphosphates constitute the natural RIG-I agonists that trigger cell-intrinsic innate immune responses during infection.

INTRODUCTION

Vertebrates possess a variety of defense mechanisms to detect, contain, and clear viral infections. Chief among these is the interferon (IFN) system, which plays a key role in inducing an antiviral state and contributes to the subsequent antigen specific adaptive immune response (Samuel, 2001). Type I IFNs (IFN-α and -β, hereafter simply referred to as IFN) and type III IFNs are induced very rapidly in all cell types by receptors that monitor the cytosol for the presence of nucleic acids indicative of virus presence. Such receptors include RIG-I-like receptors (RLRs) that recognize RNA and are themselves IFN inducible (Yoneyama and Fujita, 2009). The three members of this family—RIG-I (retinoic acid-inducible gene I), MDA5 (melanoma differentiation factor-5) and LGP-2 (laboratory of genetics and physiology-2)—all contain a DExD/H-box RNA helicase domain. RIG-I and MDA5 additionally posses two N-terminal caspase activation and recruitment domains that allow for interaction with the mitochondrial adaptor protein MAVS (Yoneyama and Fujita, 2009). MAVS triggers the activation of NF-κB, IRF-3, and IRF-7, which in turn induce transcription of IFNs and other innate response genes. Notably, mice deficient in RIG-I, MDA5, or MAVS readily succumb to infection with RNA viruses, highlighting the importance of RLRs in antiviral defense (Gitlin et al., 2006; Kato et al., 2006; Kumar et al., 2006).

Total RNA extracted from virally infected cells can stimulate specific RLRs (Hornung et al., 2006; Kato et al., 2008; Pichlmair et al., 2009). For example, RNA from cells infected with influenza A virus (flu) potently induces IFN-β when transfected into wild-type or MDA5-deficient, but not RIG-I-deficient mouse embryonic fibroblasts (Kato et al., 2008). However, the actual stimulatory RNA molecules within these pools remain largely unidentified. Instead, RLR agonists have been defined with chemically or enzymatically synthesized nucleic acids (reviewed in Schlee et al., 2009a). We and others identified RNAs transcribed in vitro by phage polymerases as potent RIG-I agonists (Hornung et al., 2006; Pichlmair et al., 2006). These RNAs carry a 5′-triphosphate (5′-PPP) moiety that is absolutely required for their activity (Hornung et al., 2006; Pichlmair et al., 2006). Other synthetic RIG-I agonists lack 5′-PPPs. These include poly I:C, which is prepared by annealing inosine and cytosine polymers that have monophosphate or diphosphate 5′ ends (Grunberg-Manago et al., 1955). Although long poly I:C activates MDA5 (Gitlin et al., 2006; Kato et al., 2006), short poly I:C (200–1000 nt) is reported to trigger RIG-I (Kato et al., 2008). Chemically synthesized RNA oligonucleotides 70 or 25 nt long and lacking 5′-PPPs also trigger RIG-I when annealed to a complementary strand (Kato et al., 2008; Takahasi et al., 2008). Thus, data obtained with synthetic RNAs suggest the possibility that there may be distinct types of RIG-I triggers in virally infected cells, including RNAs bearing 5′-PPPs or not and composed of either a single strand or two short complementary RNA strands.

In addition to synthetic RNAs, some natural RNAs also serve as RIG-I agonists. For example, RIG-I-dependent IFN production can be observed in response to transfection with genomic RNA from viruses such as flu or rabies virus that bear 5′-PPPs but not genomes of viruses that have no 5′-phosphates, such as encephalomyocarditis virus, or that have a 5′-monophosphate, such as Hantaan virus, Crimean-Congo hemorrhagic fever virus, and Borna disease virus (Habjan et al., 2008; Hornung et al., 2006; Pichlmair et al., 2006). This has led to the hypothesis that, in infected cells, RIG-I may be activated by viral genomes bearing 5′-PPPs. However, transfection of naked viral RNA does not mimic infection, and viral genomes in infected cells are in the form of viral ribonucleoprotein particles (vRNPs) in which viral proteins may prevent access of RIG-I to the RNA. For example, the flu polymerase binds to the 5′ end of the viral genome and is predicted to obscure the 5′-PPP necessary for RIG-I activation (Fodor et al., 1994; Tiley et al., 1994). Further doubt on the notion that RIG-I is primarily activated by viral genomes has come from reports that measles virus and Epstein-Barr virus transcripts (Plumet et al., 2007; Samanta et al., 2006), as well as products of host RNA cleavage by RNase L bearing 3′-monophosphates (Malathi et al., 2007), serve as the triggers for RIG-I in virally infected cells. Thus, the identification of natural RNA molecules with the potential to activate RIG-I has not clarified the identity of the actual RIG-I stimulus responsible for initiating antiviral immunity. As such, there is a pressing need to study relevant RIG-I agonists isolated from virally infected cells as opposed to characterizing the types of synthetic or natural RNA that can activate RIG-I in experimental models.

RIG-I is indispensable for IFN responses to negative-strand RNA viruses, including Sendai virus (SeV) and flu (Kato et al., 2006). SeV has a nonsegmented genome consisting of a single RNA molecule and belongs to the paramyxoviridae family. This virus family includes important human pathogens such as measles, mumps, and respiratory syncytial virus. Flu is a segmented RNA virus, and annual flu epidemics result in an estimated 250,000–500,000 deaths worldwide (Kilbourne, 2006). In addition, the ability of flu to infect different mammalian and avian species and generate reassortants constantly poses the threat that a new highly pathogenic virus will emerge, leading to a pandemic outbreak. Notably, the virulence of some flu strains is due, at least in part, to a deregulation of the innate immune response (Maines et al., 2008). Therefore, understanding how RIG-I becomes activated during infection with flu and other RNA viruses not only is of basic research interest but may also allow the development of new ways of containing viral spread and preventing disease.

Here, we characterize the RNA species responsible for activating RIG-I in cells infected with flu or SeV. Reconstitution of flu vRNPs in cell culture showed that only 5′-PPP-bearing viral genomic RNA triggered RIG-I. Furthermore, isolation of RIG-I complexes from infected cells revealed the presence of full-length viral genomes that accounted for stimulatory activity. Taken together, our data show that 5′-PPP-bearing viral genomes rather than short double-stranded RNAs, viral transcripts, or cleaved self-RNA constitute the physiological source of RIG-I stimulation and IFN induction during infection with negative-strand RNA viruses.

RESULTS

Reconstitution of Influenza A Virus vRNPs Induces IFN-α/β

To simplify the search for RIG-I agonists in flu-infected cells, we started with a mock infection system involving reconstitution of vRNPs (Fodor et al., 2002; Pleschka et al., 1996) (Figure 1A). We confirmed expression of viral RNA (vRNA), complementary RNA (cRNA), and messenger RNA (mRNA) in vRNP reconstitution experiments with each of the eight PR8 genome segments (Figure S1A available online). We then tested the IFN-inducing activity of total RNA from vRNP reconstitution experiments in an IFN-β promoter luciferase reporter assay (Figure 1B). RNA isolated from nontransfected cells (no TF) or from cells expressing the viral polymerase but no genome segment (no template) did not induce reporter activity (Figure 1B). However, RNA extracted from cells expressing the wild-type viral polymerase and any of the eight genome segments was stimulatory (Figure 1B), as reported for RNA isolated from flu-infected cells (Kato et al., 2008). Cells expressing a polymerase mutated in its active site (PB1a) did not accumulate stimulatory RNA (Figure 1C). In addition, the stimulatory activity of total cellular RNA from vRNP reconstitutions, like that of in vitro-transcribed (IVT) RNA, was RIG-I dependent (Figure 1D). The accumulation of stimulatory RNA in transfected cells was accompanied by RIG-I-dependent secretion of IFN-α/β into the culture medium, although this was not always detectable unless the cells were pretreated with IFN to upregulate RIG-I and downstream mediators prior to transfection (Figures 1E and 1F; see below for NS segment). In sum, like live infection, flu vRNP reconstitution induces RIG-I-dependent production of IFN and promotes the accumulation of RIG-I-stimulatory RNA in cells.

Transcription of vRNPs Is Dispensable for IFN Induction

Stimulatory RNA accumulated in reconstitutions with a modified template (Pleschka et al., 1996) in which the bacterial chloramphenicol acetyltransferase gene was flanked by a viral polymerase promoter composed of the 5′ and 3′ noncoding regions of the NS segment (vCAT, Figure 1C). Therefore, apart from this short promoter, specific viral sequence elements are not required for the generation of stimulatory RNA. We next asked whether transcription and/or replication are necessary. We used point mutations in the PA subunit of the viral polymerase that selectively impair one or the other process (Hara et al., 2006). As shown in Figure 2A, the PA-E410A polymerase (replication mutant) generated normal amounts of viral mRNA from an NA template but vRNA and cRNA levels were reduced about 3-fold. This was accompanied by a 3-fold reduction in IFN secretion by the transfected cells and by accumulation of lower amounts of stimulatory RNA (Figures 2B and 2C). In contrast, when transcription was selectively abrogated with the PA-D108A transcription mutant, mRNA production was blocked, yet we did not see a loss but rather observed an increase in stimulatory RNA accumulation, as well as elevated IFN secretion (Figure 2). Similar results were obtained when the PB2 genome segment was used as the template (Figure S2). Therefore, in vRNP reconstitutions, transcription is dispensable for IFN induction and for the accumulation of stimulatory RNA, which

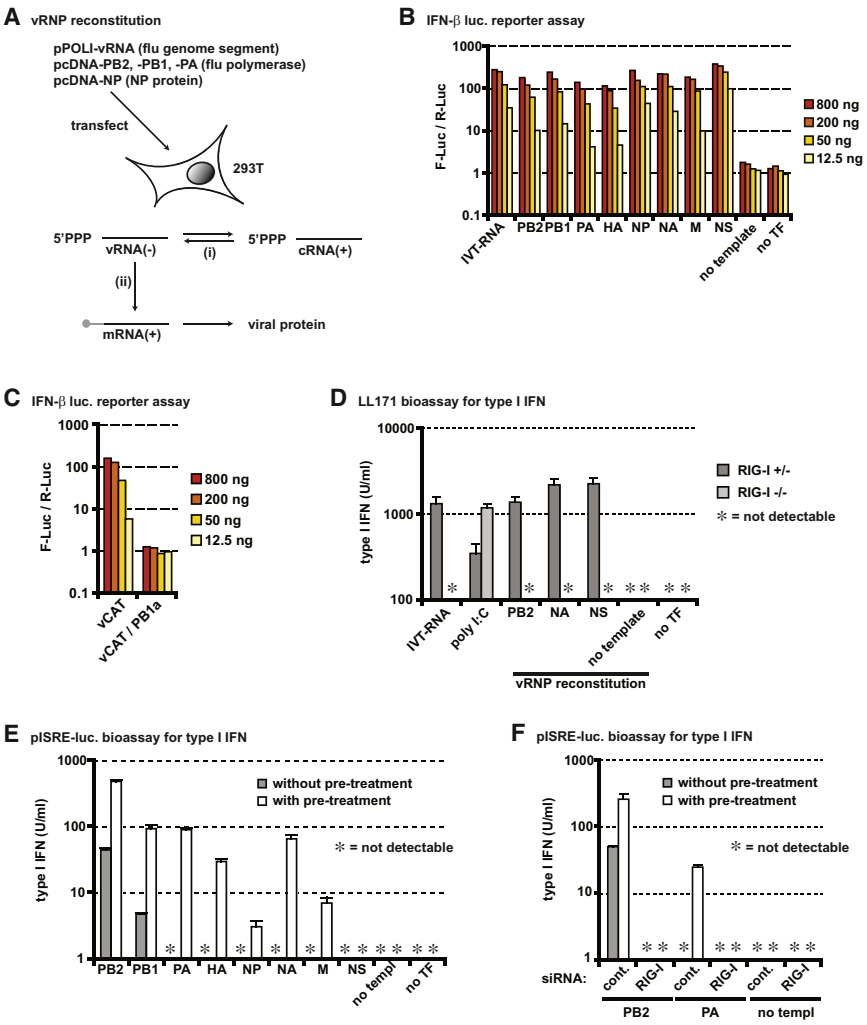

Figure 1. vRNP Reconstitution Induces IFN

(A) Scheme of the vRNP reconstitution system. Individual segments of the flu genome (vRNAs) are expressed off a promoter for RNA polymerase I, which generates uncapped RNA transcripts. These act as templates for the viral polymerase, which is expressed, together with the NP protein, from a different set of plasmids. The viral polymerase (i) replicates the negative sense genome segment via a positive sense cRNA intermediate (antigenome) and (ii) snatches short stretches of capped RNA (depicted in gray) from cellular mRNAs to serve as primers for transcription of viral mRNA, which is then translated into viral protein.

(B) Each genome segment (PB2, PB1, PA, HA, NP, NA, M, or NS) was used for the vRNP reconstitution or the genome segment was omitted (no template). Two days after transfection, total RNA was extracted and tested in an IFN-β promoter luciferase reporter assay. Results were normalized to a Renilla luciferase control and are shown as fold increase relative to cells treated with transfection reagent only. RNA extracted from non-transfected cells (no TF) and IVT-RNA (Neo^{1-99}) were included as controls.

(C) The bacterial CAT gene was flanked by viral 5′ and 3′ noncoding sequences (vCAT) and expressed instead of an authentic viral genome segment. In one group, pcDNA-PB1 was replaced by pcDNA-PB1a that encodes a mutant abrogating polymerase activity (vCAT/PB1a). Extracted RNA was tested as in (B).

(D) Mouse embryonic fibroblasts of the indicated genotype were transfected with 100 ng RNA extracted from vRNP reconstitutions with the PB2, NA, or NS genome segment. RNA from reconstitutions without a genome segment (no template), RNA from nontransfected cells (no TF), IVT-RNA (Neo^{1-99}) and poly I:C were included as controls. After overnight culture, cell culture supernatants were tested for mouse IFN content.

(E) Supernatants from vRNP reconstitutions were harvested 2 days after transfection. A bioassay was used to test for the presence of human IFN. Cells were pretreated or not with IFN-A/D (100 units/ml overnight) prior to transfection.

(F) siRNA targeting RIG-I or a control siRNA (cont.) were cotransfected with the plasmids for vRNP reconstitution. Supernatants were tested as in (E).

Representative examples of three (A–C and E) or two (D and F) independent experiments are shown. (D)–(F) show average values and standard deviation of triplicate measurements. See also Figures S1 and S7.

correlate instead with the amount of vRNA and cRNA produced by viral replication.

Full-Length Viral Genomes Bearing 5′-PPPs Trigger IFN Induction in vRNP Reconstitutions

Resistance to DNase and susceptibility to RNase V1+A treatments confirmed that extracted RNA accounted for stimulatory activity in vRNP reconstitutions (Figure 3A and Figure S3A). Digestion with Terminator (TER), a 5′-to-3′ exonuclease that degrades RNA bearing 5′-monophosphate, led to disappearance of ribosomal RNAs but did not alter the potency of the preparations (Figure 3A and Figure S3A). In contrast, treatment with calf intestinal phosphatase (CIP), which removes 5′-phosphates, completely abolished the stimulatory activity (Figure 3A and Figure S3A).

We then determined the size of the stimulatory RNA. RNA from vRNP reconstitutions using the PB2, NA, or NS segments was separated into eight fractions of decreasing size by agarose gel electrophoresis. Nucleic acid was extracted from each fraction and tested in the IFN-β reporter assay. As a control, we fractionated a 99 nt long IVT-RNA and showed that its stimulatory activity was recovered exclusively in fraction 7, as expected (Figure 3B and Figure S3B). Notably, stimulatory RNA from vRNP reconstitutions with PB2, NA, and NS segments was recovered in fractions 2, 3, and 5/6, respectively, correlating with the respective size of these segments (2341, 1413, and 890 nt). This observation excludes a dominant role for short replication intermediates (or small stimulatory RNAs of self origin), which would elute in fractions 7 or 8 (Figure 3B and Figure S3B). In sum, RNAs corresponding in size to the viral genome or antigenome and bearing more than one 5′-phosphate account for the majority of the stimulatory RNA generated during vRNP reconstitution.

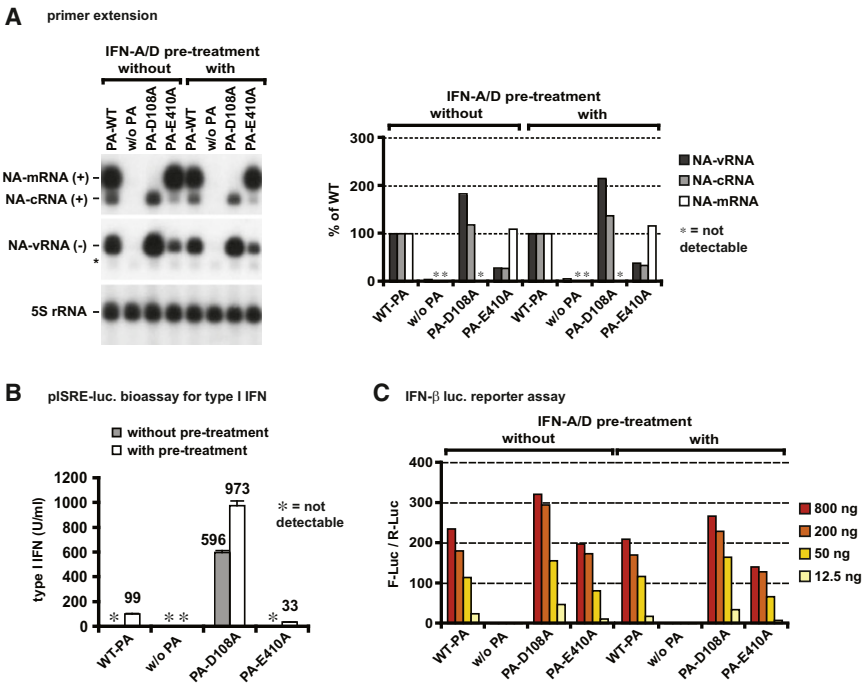

Figure 2. vRNP Replication but Not Transcription Induces IFN

(A) Cells were pretreated or not with IFN-A/D as in Figure 1E and used for vRNP reconstitution with the NA genome segment in conjunction with an intact viral polymerase (WT), a polymerase lacking the PA subunit (w/o PA), or with two point mutants, PA-D108A and PA-E410A. Extracted RNA was tested by primer extension for NA-cRNA, -mRNA, and -vRNA. A primer specific for 5S rRNA was used as a control. Signals were quantified by phosphoimager, normalized to the 5S rRNA control, and are expressed relative to WT polymerase. A nonspecific band is marked with an asterisk.

(B) Supernatants from (A) were tested in the human IFN bioassay.

(C) Total RNA extracted from (A) was tested in the IFN-β reporter assay.

(A) is representative of two independent experiments, and (B) and (C) of four experiments. (B) shows average values and standard deviation of triplicate measurements. See Figure S2 for equivalent experiments using the PB2 genome segment.

NS1 Inhibits IFN Induction in vRNP Reconstitutions and Associates with RIG-I and Stimulatory RNA

The NS segment encodes the viral NS1 and NS2 proteins, the former of which binds RNA and, in the PR8 strain, acts as an inhibitor of IFN induction (Gack et al., 2009; Guo et al., 2007; Mibayashi et al., 2007; Opitz et al., 2007; Pichlmair et al., 2006). Accordingly, we did not detect secretion of IFN in vRNP reconstitutions using the NS genome segment (Figure 1E) even though stimulatory RNA accumulated in these cells (Figure 1B and Figure S3A). However, when we modified the PR8 NS genome segment by introducing two point mutations (R38A and K41A) in the sequence encoding the RNA binding domain (Donelan et al., 2003), vRNP reconstitution resulted in secretion of significant amounts of IFN (Figures S1B–S1E). These results show that, as expected, NS1 inhibits IFN induction during vRNP reconstitution.

To explore the possibility that IFN inhibition involves simultaneous binding of NS1 to stimulatory RNAs and to RIG-I, we used a two-step immunoprecipitation approach (Figure S4A). Lysates from cells expressing NS1 and FLAG-tagged RIG-I were combined with IVT-RNA, and RIG-I complexes were precipitated with α-FLAG antibodies. As described (Pichlmair et al., 2006), wild-type NS1 but not the NS1 R38A/K41A mutant associated with RIG-I (Figure S4B). Next, native complexes were eluted using FLAG peptide and were reprecipitated with α-NS1 antibody (Figure S4C). The majority of the stimulatory RNA was

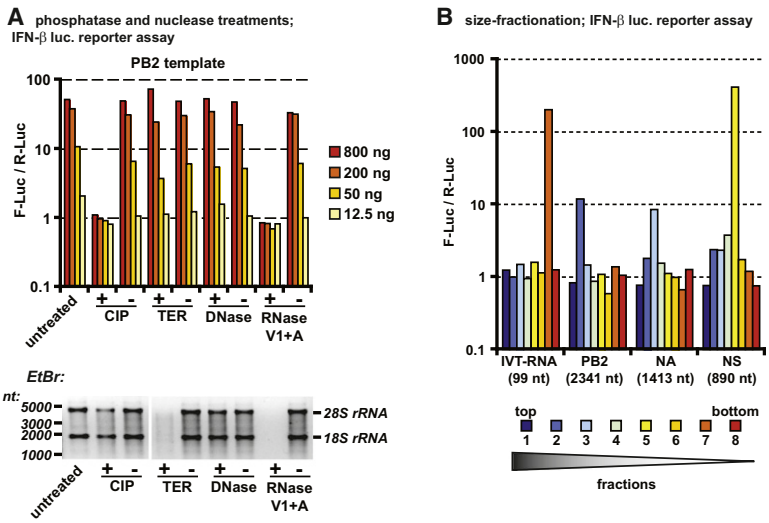

Figure 3. Full-Length Viral Genomes Trigger IFN Induction in vRNP Reconstitutions

(A) RNA extracted from reconstitutions using the PB2 genome segment was subjected to CIP, TER, DNase, or RNase A+V1 digestion. Parallel reactions with (+) and without (−) enzyme were performed and RNAs were analyzed by gel electrophoresis and ethidium bromide staining (bottom) and in the IFN-β reporter assay (top). Extracted RNA without any further treatment was also included (untreated).

(B) RNA extracted from reconstitutions using the PB2, NA, or NS genome segments was size fractionated on agarose gels (fractions 1 to 8 from the pockets to the bottom). RNA was reisolated and tested as in (A). IVT-RNA (Neo^{1-99}) was included in the fractionation. The length of this RNA and that of the viral genome segments is given in brackets.

Data are representative of three independent experiments. See also Figure S3.

retained in the second immunoprecipitation with wild-type NS1 (Figure S4D), indicating that the viral protein traps stimulatory RNA and RIG-I in a trimolecular complex. However, RIG-I was not necessary for NS1-dependent sequestration of stimulatory RNA as the latter still occurred in RIG-I-deficient cells (Figure S4E).

Association with NS1 Marks the Natural RIG-I Agonist during Flu Infection

The above experiments suggested that NS1 immunoprecipitation might allow the isolation of RIG-I agonists from flu-infected cells. Indeed, nucleic acids extracted from NS1 pulldowns from flu-infected cells potently induced the IFN-β reporter (Figure 4A). This approach did not require artificial overexpression of any protein and allowed quantitative recovery of all relevant RIG-I agonists as evidenced by the fact that it depleted cell lysates from stimulatory activity (Figure 4B). The stimulatory activity of NS1-associated RNAs was sensitive to RNase A treatment but not DNase digestion and was RIG-I dependent as it was greatly diminished by siRNA depletion of mouse but not human RIG-I in NIH 3T3 cells and vice versa in HEK293T cells (Figure S4F and Figure 4C). We conclude that RIG-I agonistic RNAs generated during flu infection are associated with NS1 and can be purified from infected cells by NS1 immunoprecipitation.

Flu Genomes Constitute the Physiological RIG-I Agonist

NS1-associated stimulatory activity was sensitive to CIP but not to TER treatment and encompassed RNA species ranging from 0.5 to 6 kb (Figures 5A and 5B). The phosphatase sensitivity and size characteristics suggested that stimulatory activity might be attributable to 5′-PPP-containing genomic or antigenomic RNA segments. Indeed, primer extension analysis revealed that all eight negative sense genome segments were highly enriched in the NS1 but not a control immunoprecipitate (Figures 5C and 5D). For example, PB2 vRNA was 21-fold enriched among NS1 associated RNAs compared to RNA extracted from the lysate (Figures 5C and 5D). We also detected some viral cRNA and mRNA in the NS1 precipitate, albeit not for all segments (Figures 5C and 5D). In northern blots with a full-length probe for M segment vRNA, the NS1-associated RNA migrated at around 1000 nt, corresponding to the size of the genome segment (1027 nt, Figure 5E). Thus, full-length flu genomes are highly enriched in the NS1-associated RIG-I stimulatory fraction.

To validate these findings by an independent approach, we generated a cell line expressing FLAG-tagged RIG-I and infected these cells with PR8 flu or a mutant that does not express the NS1 protein (ΔNS1). RIG-I was precipitated with α-FLAG antibody, and associated nucleic acids were tested in the IFN-β promoter reporter assay (Figure 6A). We recovered stimulatory RNA from the FLAG immunoprecipitation but not from a control reaction (Figure 6A and Figure S5A). Consistent with the observations from vRNP reconstitution and NS1 precipitation experiments, RIG-I-associated RNA lost its stimulatory activity after CIP but not TER treatment (Figure 6B). We characterized RNA from RIG-I precipitates by three approaches. First, we used oligonucleotides complementary to the PB2 and NA segments in primer extension experiments. We found that both vRNAs and cRNAs were retained specifically in the RIG-I purification,

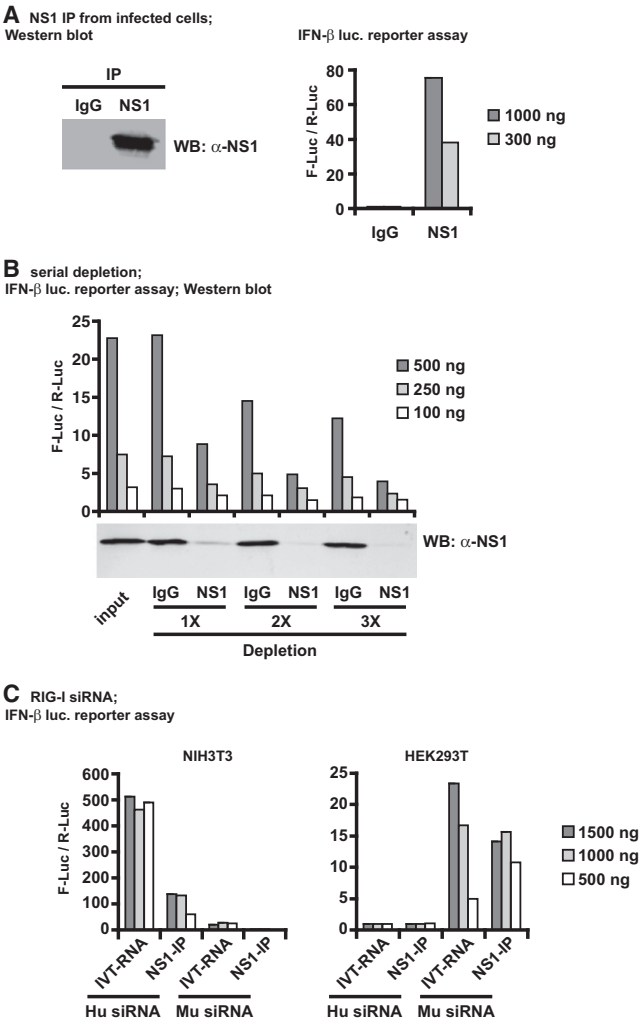

Figure 4. NS1 Associates with the Actual RIG-I Agonist during Flu Infection

(A) NS1 was immunoprecipitated from total lysate of MDCK cells infected with PR8 WT flu for 48 hr at a multiplicity of infection (MOI) of 0.01. Nucleic acids associated with control IgG or NS1 immunoprecipitates (IP) were extracted and tested in the IFN-β reporter assay. Western blot (WB) shows the presence of NS1.

(B) Total lysate of MDCK cells infected with flu was subjected to three rounds of mock or NS1 immunoprecipitation. Nucleic acids were extracted from the lysate and the depleted fractions and tested as in (A). The depletion of NS1 was monitored by WB.

(C) Mouse NIH 3T3 or human HEK293T cells were cotransfected with the IFN-β promoter reporter plasmid and siRNAs specific for human or mouse RIG-I. After 48 hr, cells were transfected with the indicated amount of IVT-RNA or NS1-associated RNA (NS1-IP), and luciferase activity was measured 12 hr later.

(A), (B), and (C) are representative of five, three, and two independent experiments, respectively. See also Figure S4.

while contaminating 5S rRNA was detectable in both RIG-I and control precipitates (Figure 6C). Second, in northern blots for vRNA of the M segment, the RIG-I-associated RNA migrated at the size expected for the full-length genome segment (1027 nt), and we did not detect faster-migrating RNA species (Figure 6D). Third, the size profile of RIG-I-associated stimulatory

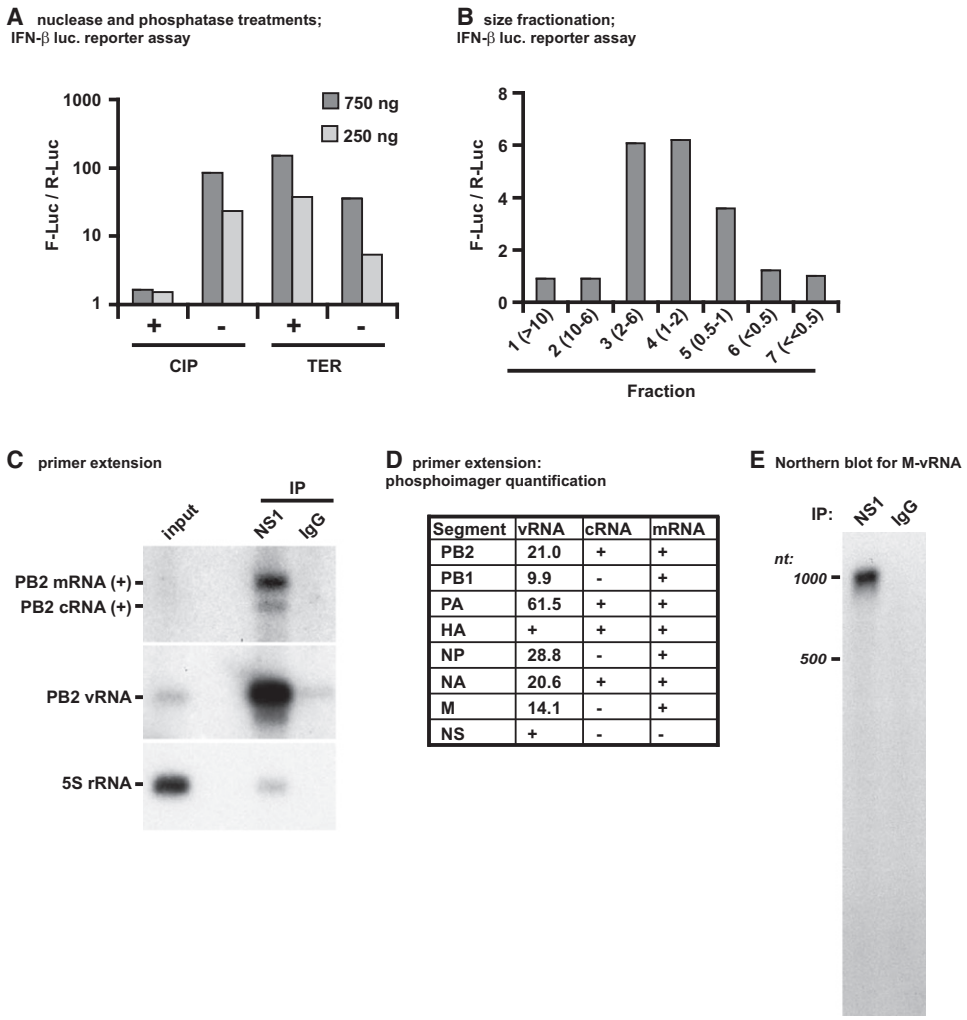

Segment	vRNA	cRNA	mRNA
PB2	21.0	+	+
PB1	9.9	-	+
PA	61.5	+	+
HA	+	+	+
NP	28.8	-	+
NA	20.6	+	+
M	14.1	-	+
NS	+	-	-

Figure 5. NS1 Binds 5′-PPP Influenza A Virus Genomes and Antigenomes

(A) NS1 associated stimulatory nucleic acid (see Figure 4A) was subjected to CIP or TER treatment and tested in the IFN-β reporter assay.

(B) Size profile of the NS1-associated stimulatory RNA. NS1-associated nucleic acid (see Figure 4A) was resolved by agarose gel electrophoresis. The gel was cut into seven fractions, and RNA was re-extracted and analyzed as in (A). The relative molecular weight of each fraction in nucleotides (×1000) is based on comparison with an RNA marker.

(C) NS1-associated RNA was immunoprecipitated from infected cells and PB2 mRNA, cRNA, and vRNA as well as 5S rRNA were detected by primer extension. For all fractions, the same amount of RNA (400 ng) was used.

(D) The primer extension shown in (C) was repeated with oligonucleotides complementary to all other segments and quantified by phosphoimager analysis. Results are expressed as fold enrichment in the NS1 precipitate compared to input RNA. HA and NS vRNAs and some mRNAs and cRNAs were present in the NS1 precipitate (denoted by the "plus" sign), but not detectable in the input material, hence fold enrichments could not be calculated.

(E) Northern blot analysis of RNA associated with α-NS1 or control antibody using a full-length, internally labeled probe specific to M-vRNA.

(A)–(E) show representative examples of two independent experiments.

RNA matched the size range of flu genome segments (890–2341 nt) and was not found in smaller fractions (Figure 6E). Thus, direct RIG-I precipitation reveals only the presence of flu viral genomes and not other stimulatory nucleic acids in flu-infected cells.

RIG-I Is Triggered by Viral Genomic RNA during Sendai Virus Infection

To extend our findings to other viruses sensed by RIG-I, we chose SeV. The SeV genome consists of a single negative sense 5′-PPP-bearing RNA molecule 15,384 nt long that serves as a template for the synthesis of capped mRNAs and 5′-PPP antigenomes. Unlike flu, SeV makes short (~50 nt long) leader and trailer 5′-PPP RNAs during infection. Thus, in SeV-infected cells, these RNAs could serve as RIG-I agonists, as proposed for the related measles virus (Plumet et al., 2007).

Total RNA from SeV-infected cells but not from uninfected cells potently induced the IFN-β promoter upon transfection into reporter cells (Figure 7A). As for flu, stimulatory activity was RIG-I dependent and sensitive to RNase, but not DNase treatment (Figures S6A and S6B) and was additionally sensitive

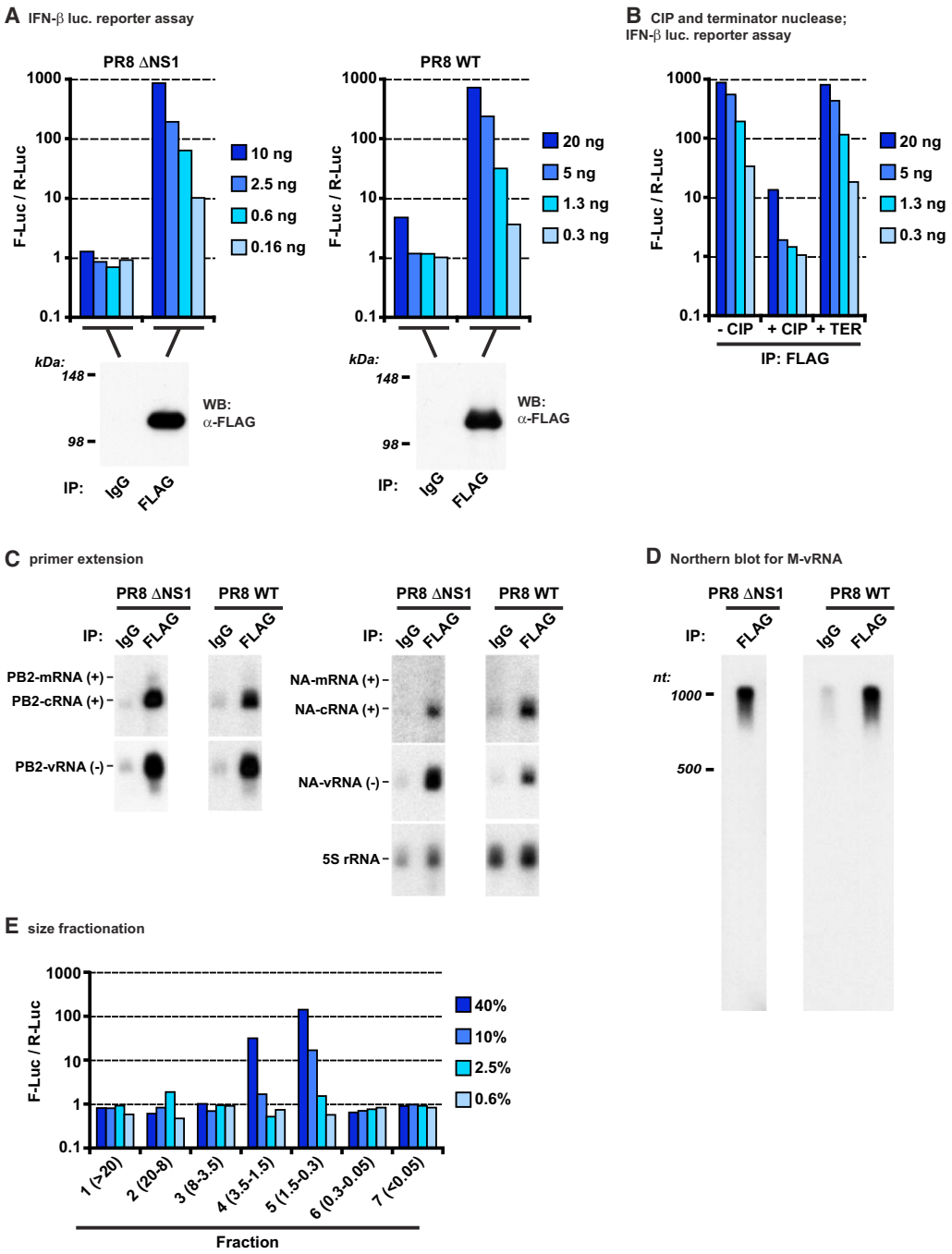

Figure 6. Influenza A Virus Genomes and Antigenomes Trigger IFN Induction during Infection

(A) HEK293 cells expressing FLAG-RIG-I were infected with flu PR8 WT or PR8 ΔNS1 at an MOI of 1. After 16 hr, RIG-I was precipitated with α-FLAG antibody. An isotope matched antibody (IgG) was used as a control. RNA extracted from the precipitates was tested in the IFN-β reporter assay (top). The precipitates were also tested by WB using α-FLAG antibodies (bottom).

(B) RNA associated with FLAG-RIG-I (from PR8 ΔNS1 infection) was analyzed by CIP and TER treatment and tested as in (A).

(C) Stimulatory RNA in the control and FLAG-RIG-I precipitates was analyzed by primer extension for the presence of PB2 and NA mRNA, cRNA, and vRNA, as well as 5S rRNA.

(D) Northern blot analysis of RNA bound to FLAG-RIG-I using a full-length probe specific for M-vRNA.

(E) Size profile of the FLAG-RIG-I associated stimulatory RNA (from PR8 ΔNS1 infection) determined as in Figure 5B.

(A) and (B)–(E) are representative examples of four and two independent experiments, respectively. See also Figures S5 and S7.

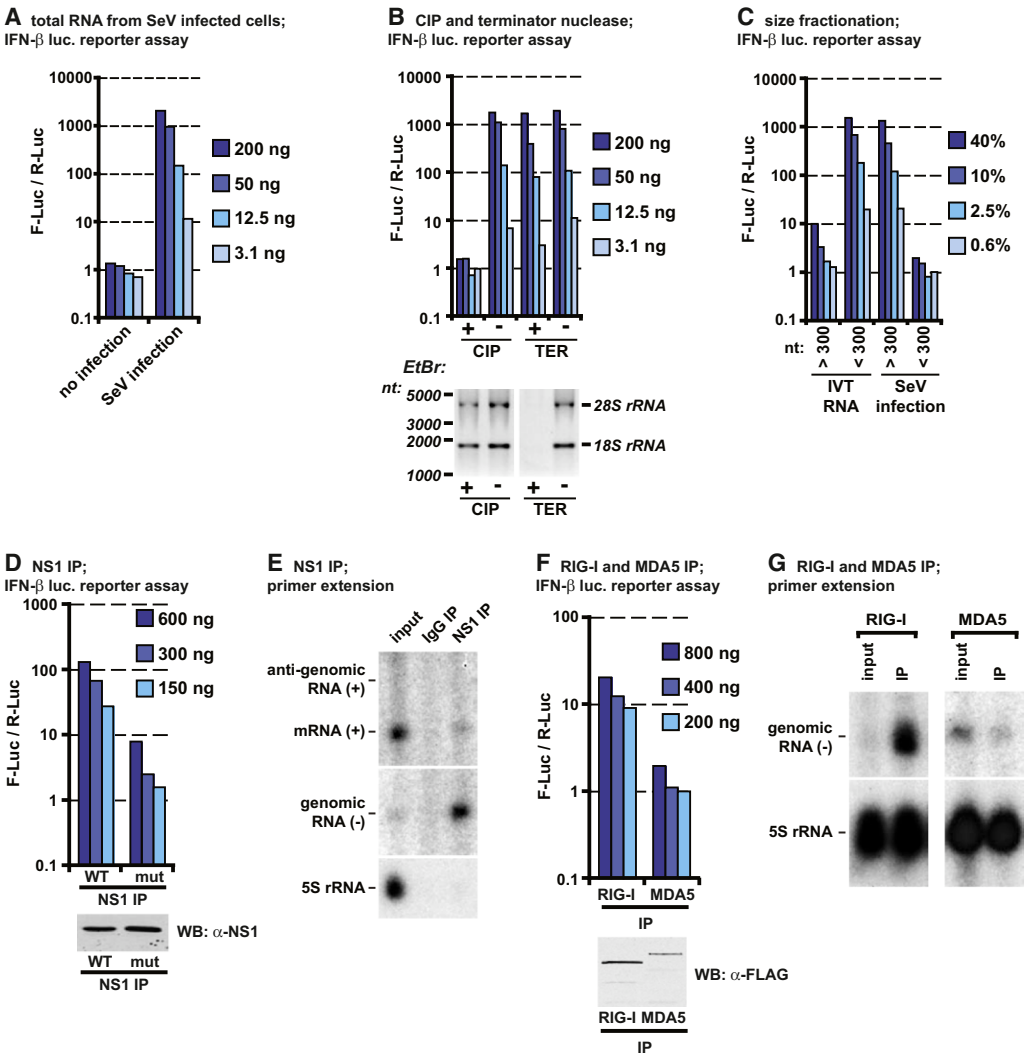

Figure 7. Viral Genomes Constitute the Primary RIG-I Agonist during Sendai Virus Infection

(A) HEK293 cells were infected or not with SeV at an MOI of 5. After 16 hr, RNA was extracted with TRIZOL and tested in the IFN-β reporter assay as in Figure 1B.

(B) Stimulatory RNA extracted from SeV-infected cells was treated with CIP or TER. The minus sign denotes a control reaction without enzyme. Aliquots were tested as in (A) (top) and by agarose gel electrophoresis and ethidium bromide staining (bottom).

(C) Size profile of stimulatory RNA extracted from SeV-infected cells. RNA from (A) was resolved by agarose gel electrophoresis. The gel was cut into two fractions, corresponding to RNAs migrating above or below 300 nt by comparison with an RNA marker. RNA was re-extracted and analyzed as in (A). IVT-RNA (Neo^{1-99}, 99 nt) was included as a control.

(D) HEK293T cells were transfected with plasmids expressing NS1 or NS1-R38A/K41A. After 24 hr, cells were infected with SeV at an MOI of 5. Cell lysates were prepared 20 hr later, and NS1 was precipitated. The precipitates were analyzed by WB (bottom) and nucleic acids were extracted and tested as in (A) (top).

(E) Transiently transfected HEK293T expressing NS1 were infected with SeV and NS1 was precipitated as in (D). Nucleic acid extracted from the cell lysate (input) or associated with α-NS1 or IgG control antibodies (IP) was analyzed for the presence of SeV genomic, antigenomic, and messenger RNA and 5S rRNA by primer extension.

(F) FLAG-RIG-I and FLAG-MDA5 were expressed in HEK293T cells by transient transfection, followed by infection with SeV after 24 hr. Cell lysates were prepared after 20 hr and RIG-I and MDA5 were precipitated using α-FLAG antibodies. Nucleic acids were extracted from precipitates (IP) and analyzed as in (A) (top panel). The bottom panel shows a WB using an aliquot of the IP.

(G) Nucleic acids extracted from cell lysates (input) and precipitates (IP) as in Figure 7F were tested by primer extension for SeV genomic RNA and 5S rRNA.

Panels (A), (C), (F), and (G) and panels (B), (D), and (E) are a representative examples of three and two independent experiments, respectively. See also Figures S6 and S7.

to CIP but not TER (Figure 7B). Size fractionation into "large" (>300 nt) and "small" (<300 nt) RNAs showed that stimulatory RNA from SeV infected cells was "large," whereas that of a control 99 nt IVT RNA was "small" (Figure 7C). This excludes a major role for leader and trailer RNAs in triggering RIG-I and together with the CIP sensitivity suggests that genomic and/or antigenomic RNA is the primary RIG-I agonist during SeV infection.

To capture the physiologically relevant RIG-I agonist during SeV infection, we again made use of flu NS1, which is able to inhibit IFN responses to SeV (Wang et al., 2000). As predicted, WT NS1 but not the NS1 mutant was able to precipitate stimulatory RNAs from extracts of transiently transfected cells infected with SeV (Figure 7D). We next tested by primer extension if NS1-associated stimulatory RNA contains SeV genomic, antigenomic, and/or messenger RNA (Figure S6D). Compared to RNA extracted from the cell lysate, SeV genomic RNA was enriched between 6.6- and 11.5-fold in the NS1 precipitate, while the antigenome and N-mRNA were not detectable (Figure 7E and Figure S6C). We validated these results by precipitating FLAG-RIG-I (or FLAG-MDA5 as a control) from transiently transfected cells infected with SeV. Stimulatory RNA was recovered only in the FLAG-RIG-I immunoprecipitation and SeV genomic RNA was enriched between 7.4- and 17-fold in the RIG-I precipitate compared to cell lysate (Figures 7F and 7G). Thus, flu NS1 or RIG-I precipitation selectively enriches for SeV viral genomes. Taken together with the size characteristics of the stimulatory RNA and the CIP sensitivity, these observations show that 5′-PPP bearing genomic RNA is the main trigger for RIG-I during SeV infection.

DISCUSSION

Sensing of virus presence and cytokine induction via the RIG-I pathway are crucial for successful host defense against infections with RNA viruses (Pichlmair and Reis e Sousa, 2007; Yoneyama and Fujita, 2009). Although the signaling cascade from RIG-I to IFN induction is well defined, the identity and properties of RIG-I agonists and the mechanisms that allow the helicase to be activated specifically in infected cells are controversial. Viral genomes, shorter viral transcripts, double-stranded RNA, or cellular RNA cleaved by RNase L have all been suggested to trigger RIG-I (Habjan et al., 2008; Hausmann et al., 2008; Hornung et al., 2006; Kato et al., 2008; Malathi et al., 2007; Pichlmair et al., 2006; Plumet et al., 2007; Ranjith-Kumar et al., 2009; Samanta et al., 2006; Takahasi et al., 2008). Such RNAs have been variably defined as containing no phosphates, 5′-monophosphates, 5′-triphosphates, or 3′-monophosphates (Hornung et al., 2006; Kato et al., 2008; Malathi et al., 2007; Pichlmair et al., 2006; Takahasi et al., 2008) and, in some cases, to require specific structural determinants or sequence motifs (Marques et al., 2006; Saito et al., 2008; Schlee et al., 2009b; Schmidt et al., 2009; Uzri and Gehrke, 2009). Most of these studies, however, have been limited to the analysis of RIG-I activation by defined RNAs, including synthetic RNAs made by chemical or enzymatic synthesis or vRNAs isolated from virus particles. Although such studies have been instrumental in defining the range of RNAs that can activate RIG-I, they have fallen short of identifying physiological RIG-I agonists that are actually responsible for activating RIG-I and triggering IFN production in virus-infected cells. Here, we analyze the properties of relevant RIG-I agonists in cells infected with flu or SeV. Using three complementary approaches, we find that genomic RNA generated by viral replication constitutes the major trigger for RIG-I and conclude that viral transcripts, RNase L cleavage products, and/or other RNA species make only a minor contribution to cell-intrinsic antiviral innate immunity.

We started with a mock infection system that allows the reconstitution of flu vRNP complexes and leads to IFN induction and accumulation of stimulatory RNA (Figure 1). Using this system, we found that an artificial genome segment that retains the viral promoter but otherwise lacks viral sequences behaved similarly to bona fide flu vRNA segments (Figure 1C). Therefore, RIG-I activation in this setting is largely sequence independent. This is in contrast to recent reports suggesting that a polyuridine motif in the hepatitis C virus 3′ untranslated region is required for triggering RIG-I (Saito et al., 2008; Uzri and Gehrke, 2009). Importantly, those conclusions were based on cellular responses to transfected IVT-RNAs, whereas the vRNP reconstitution system used here allowed us to look at RNAs made endogenously by the mock-infected cell. Nevertheless, it remains possible that sequence motifs may facilitate RIG-I activation in some instances. Indeed, such motifs could contribute to the observed quantitative differences in accumulation of stimulatory RNA and IFN secretion depending on which of eight flu genome segments was used for reconstitution (Figures 1B and 1E). Alternatively, those differences may be due to the expression of viral proteins associated with the viral genome (such as the PB2, PB1, PA, NP, M1, NS1, and NS2 proteins), which may inhibit or facilitate the access and/or function of RIG-I.

In a particularly striking example of the latter point, the viral NS1 protein completely blocked IFN induction during vRNP reconstitution (Figures S1B–S1E). NS1 can interact with RIG-I (Mibayashi et al., 2007), especially in the presence of stimulatory RNA through formation of a trimeric complex (Figures S4A–S4D) (Pichlmair et al., 2006). This activity of NS1 is dependent on the integrity of the RNA binding domain, which is reported to bind double-stranded RNA (Hatada and Fukuda, 1992). Interestingly, recent studies demonstrate that, in addition to the 5′-PPP, synthetic RNAs require base pairing at the 5′ end in order to trigger RIG-I (Schlee et al., 2009b; Schmidt et al., 2009). Such 5′ base-paired regions can be found within the genomes of flu and SeV (Knipe and Howley, 2007). We therefore envisage that one mechanism of NS1 action may be to bind to the base-paired region at the 5′ end of viral genomes. This does not prevent RIG-I binding to the 5′-PPP via its C-terminal domain (Cui et al., 2008; Takahasi et al., 2008) but may block translocation along the base paired stretch, which has been proposed to be necessary for signaling (Myong et al., 2009). This model (Figure S4G) therefore suggests that the ability of NS1 to associate with stimulatory RNAs is due to its propensity to recognize RNA secondary structure determinants important for RIG-I activation (Schlee et al., 2009b; Schmidt et al., 2009) and is consistent with the finding that NS1 binds agonistic RNA in the absence of functional RIG-I (Figure S4E). This model does not exclude additional modes of NS1 action, such as inhibition of TRIM25-mediated RIG-I ubiquitination (Gack et al., 2009).

Given the finding that NS1 associates with stimulatory RNA, we used it as one of our strategies to purify RIG-I agonists from infected cells. As a complementary approach, we immunoprecipitated epitope-tagged RIG-I from infected cells. Both precipitations enriched for flu and SeV genomic RNAs. Furthermore, NS1- or RIG-I-associated stimulatory RNA matched the

size of vRNA and required 5′-phosphates for stimulatory activity. Thus, viral genomic RNAs represent the major RIG-I agonist in flu- and SeV-infected cells. Antigenomes, which have an identical size to the genome and also bear 5′-PPP, may also contribute to IFN induction. Indeed, flu cRNAs were present in the NS1 and RIG-I immunoprecipitates (Figures 5C, 5D, and 6C). Their contribution, however, is likely to be minor, as cRNA accumulates to much lower levels compared to vRNA (Robb et al., 2009) (Figure S1A and Figure 5C).

In contrast to vRNA and cRNA, flu or SeV transcripts do not appear to trigger RIG-I, based on the size distribution of the stimulatory RNA, the fact that the transcription-defective PA-D108A mutant flu polymerase was fully capable of inducing IFN in vRNP reconstitution experiments, and the fact that viral mRNAs, like cellular mRNAs, are capped. These findings do not exclude a role for viral transcripts in activating RIG-I in other virus infections such as measles virus and Epstein-Barr virus (Plumet et al., 2007; Samanta et al., 2006) as those viruses use mechanisms for transcription that can result in transcripts bearing 5′-triphosphates. However, it is worth noting that measles-related SeV also generates uncapped short 5′-triphosphate-bearing leader and trailer RNA transcripts, yet our size fractionation experiments exclude a role for these short RNAs in RIG-I stimulation in SeV-infected cells (Figure 7C). We speculate that leader and trailer RNAs lack a sufficient degree of secondary structure to potently trigger RIG-I and/or are sequestered by association with cellular proteins. Similarly, during infection with another paramyxovirus, respiratory syncytial virus, leader RNAs do not play an important role in IFN induction (Bitko et al., 2008). Thus, the ability of a virus to generate uncapped transcripts during its life cycle does not necessarily mean that these will act as RIG-I agonists.

Our results also appear to exclude RNase L cleavage products as major RIG-I agonists during infection with negative-strand RNA viruses. Such cleavage products have 5′-hydroxyl and 3′-monophosphate ends and are expected to be shorter than 200 nt (Malathi et al., 2007; Wreschner et al., 1981). Yet we found that the stimulatory activity of RNA isolated from both vRNP reconstitutions and infected cells strictly required 5′-phosphates and was longer than 200 nt. It may therefore be the case that RNase L-cleaved self or viral RNAs are not obligate RIG-I agonists but primarily serve to amplify RIG-I activation driven by vRNA. Consistent with such a model, RNase L-deficient mice show only a 6-fold reduction in serum IFN-β after infection with SeV (Malathi et al., 2007).

Virus entry into cells can induce innate immune responses in the absence of replication (Collins et al., 2004) and, in fact, 56°C-inactivated influenza virus was originally used to discover IFNs (Isaacs and Lindenmann, 1957). In retrospect, the latter observations may be explained by RIG-I-mediated recognition of incoming viral genomes delivered by high doses of fusogenic virus. However, the fact that NS1, a nonstructural protein only produced after infection, can effectively prevent IFN induction by flu indicates that the incoming genomes of virus particles are not the major triggers of RIG-I activation during live infection. Consistent with that notion, infection in the presence of drugs that block translation (and, consequently, inhibit the virus life cycle) prevents accumulation of stimulatory RNA in the cytoplasm of flu-infected cells (Figure S7A). Therefore, we believe that progeny genomes are the likely source of RIG-I stimulatory activity. However, flu replication is confined to the nucleus (Jackson et al., 1982; Krug et al., 1987), raising the question of how progeny viral genomic RNA is sensed in the cytoplasmic compartment monitored by RIG-I. It is clear that progeny genomes traverse the cytoplasm for assembly of new virions, but these genomes are bound at the ends by the flu polymerase and along their length by the NP protein. For RIG-I to interact with the genome and the critical 5′-PPP moiety, these viral proteins need either to be displaced or to dissociate from the vRNA. The former process could be facilitated by the ATP-driven helicase activity of RIG-I (Takahasi et al., 2008), whereas the latter may occur naturally as part of an equilibrium reaction. Indeed, viral RNA within vRNPs is accessible to nucleases (Duesberg, 1969) and might therefore also permit RIG-I docking, at least for a fraction of the estimated 100,000 viral genome segments present within an infected cell.

Here, we report that viral genomes are the major trigger for RIG-I in cells infected with negative-sense single-stranded RNA viruses. Our findings confirm earlier suggestions that single stranded RNAs bearing 5′-PPPs constitute effective agonists for RIG-I (Hornung et al., 2006; Pichlmair et al., 2006). It is worth noting that single-strandedness does not mean absence of base pairing. Flu genome segments and SeV genomic RNA adopt a "panhandle" conformation by pairing of complementary 5′ and 3′ ends (Knipe and Howley, 2007). Interestingly, Myong et al. showed that RIG-I translocates on synthetic double-stranded RNA molecules and that this movement is enhanced the presence of 5′-PPP (Myong et al., 2009). Notably, treatment of the stimulatory RNAs studied here with the double-stranded RNA specific nuclease RNase III abolishes RIG-I stimulatory activity (Figure S7B), which indicates that these RNAs contain base-paired regions. Therefore, we envisage that base-pairing within the "panhandle" structure of single-stranded flu and SeV genomic RNAs acts in cooperation with the presence of 5′-PPP to allow for potent RIG-I activation (Pichlmair et al., 2006). This model is likely to apply to other viruses sensed by RIG-I as panhandle structures are found in many single stranded RNA virus genomes (Schlee et al., 2009b). Thus, RIG-I integrates RNA secondary structure determinants and the presence of a 5′-PPP to effectively discriminate viral genomes from self-RNA.

EXPERIMENTAL PROCEDURES

Reconstitution of Flu vRNPs

One million HEK293T cells were transiently transfected using lipofectamine 2000 (Invitrogen) with 1 μg each of pcDNA-PB2, -PB1, -PA, and -NP (all from the flu WSN strain) and a pPOLI construct expressing a flu genome segment (derived from the flu A/PR/8/34 [PR8] strain). Two days after transfection, cell culture supernatants were collected and total RNA was extracted with TRIZOL (Invitrogen).

RNA Analysis

CIP (New England Biolabs), TER (Epicenter Biotechnologies), RQ1 DNase (Promega), and RNase V1 (Ambion) combined with RNase A (Sigma) or RNase III (Ambion) were used according to manufacturer recommendations. A control reaction omitting the enzyme was carried out in parallel. RNA was recovered by extraction with phenol:chloroform:isoamylalcohol (25:24:1), followed by chloroform extraction and precipitation with ethanol and sodium acetate in

the presence of glycogen. For size fractionation, RNAs were separated on 0.75% TBE-agarose gels at 70 V for 3 hr. Gels were cut into slices (including the well and bottom of the gel) and RNA was recovered from gel pieces with Quantum Prep Freeze N Squeeze Spin Columns (Bio-Rad) and precipitation (as above). Primer extension and northern blot assays are described in the Extended Experimental Procedures. Oligonucleotide sequences are given in Table S1.

Immunoprecipitation from Virally Infected Cells

Lysates from cells infected with flu PR8, flu PR8 ΔNS1, or SeV were used for immunoprecipitation as detailed in the Extended Experimental Procedures. Aliquots of the beads were boiled in SDS sample buffer for western blot analysis or RNA was recovered from the beads by extraction and precipitation as described above.

SUPPLEMENTAL INFORMATION

Supplemental Information includes Extended Experimental Procedures, seven figures, and one table and can be found with this article online at doi:10.1016/j.cell.2010.01.020.

ACKNOWLEDGMENTS

We thank Peter Palese and Shizuo Akira for reagents and George Brownlee and all members of the Immunobiology laboratory for advice and critical discussions. J.R. is a recipient of FEBS and Human Frontier Science Program long-term fellowships. D.G. is a recipient of a Baxter and Alma Ricard Foundation scholarship. K.B. is a recipient of a Biotechnology and Biological Sciences Research Council studentship. E.F. is supported by grants from the MRC, Wellcome Trust, and the European Union (FLUINNATE). Work in the C.R.S. laboratory is funded by Cancer Research UK and a prize from Fondation Bettencourt-Schueller.

Received: June 1, 2009
Revised: November 1, 2009
Accepted: January 6, 2010
Published: February 4, 2010

REFERENCES

Bitko, V., Musiyenko, A., Bayfield, M.A., Maraia, R.J., and Barik, S. (2008). Cellular La protein shields nonsegmented negative-strand RNA viral leader RNA from RIG-I and enhances virus growth by diverse mechanisms. J. Virol. *82*, 7977–7987.

Collins, S.E., Noyce, R.S., and Mossman, K.L. (2004). Innate cellular response to virus particle entry requires IRF3 but not virus replication. J. Virol. *78*, 1706–1717.

Cui, S., Eisenächer, K., Kirchhofer, A., Brzózka, K., Lammens, A., Lammens, K., Fujita, T., Conzelmann, K.K., Krug, A., and Hopfner, K.P. (2008). The C-terminal regulatory domain is the RNA 5′-triphosphate sensor of RIG-I. Mol. Cell *29*, 169–179.

Donelan, N.R., Basler, C.F., and García-Sastre, A. (2003). A recombinant influenza A virus expressing an RNA-binding-defective NS1 protein induces high levels of beta interferon and is attenuated in mice. J. Virol. *77*, 13257–13266.

Duesberg, P.H. (1969). Distinct subunits of the ribonucleoprotein of influenza virus. J. Mol. Biol. *42*, 485–499.

Fodor, E., Pritlove, D.C., and Brownlee, G.G. (1994). The influenza virus panhandle is involved in the initiation of transcription. J. Virol. *68*, 4092–4096.

Fodor, E., Crow, M., Mingay, L.J., Deng, T., Sharps, J., Fechter, P., and Brownlee, G.G. (2002). A single amino acid mutation in the PA subunit of the influenza virus RNA polymerase inhibits endonucleolytic cleavage of capped RNAs. J. Virol. *76*, 8989–9001.

Gack, M.U., Albrecht, R.A., Urano, T., Inn, K.S., Huang, I.C., Carnero, E., Farzan, M., Inoue, S., Jung, J.U., and García-Sastre, A. (2009). Influenza A virus NS1 targets the ubiquitin ligase TRIM25 to evade recognition by the host viral RNA sensor RIG-I. Cell Host Microbe *5*, 439–449.

Gitlin, L., Barchet, W., Gilfillan, S., Cella, M., Beutler, B., Flavell, R.A., Diamond, M.S., and Colonna, M. (2006). Essential role of mda-5 in type I IFN responses to polyriboinosinic:polyribocytidylic acid and encephalomyocarditis picornavirus. Proc. Natl. Acad. Sci. USA *103*, 8459–8464.

Grunberg-Manago, M., Oritz, P.J., and Ochoa, S. (1955). Enzymatic synthesis of nucleic acidlike polynucleotides. Science *122*, 907–910.

Guo, Z., Chen, L.M., Zeng, H., Gomez, J.A., Plowden, J., Fujita, T., Katz, J.M., Donis, R.O., and Sambhara, S. (2007). NS1 protein of influenza A virus inhibits the function of intracytoplasmic pathogen sensor, RIG-I. Am. J. Respir. Cell Mol. Biol. *36*, 263–269.

Habjan, M., Andersson, I., Klingström, J., Schümann, M., Martin, A., Zimmermann, P., Wagner, V., Pichlmair, A., Schneider, U., Mühlberger, E., et al. (2008). Processing of genome 5′ termini as a strategy of negative-strand RNA viruses to avoid RIG-I-dependent interferon induction. PLoS ONE *3*, e2032.

Hara, K., Schmidt, F.I., Crow, M., and Brownlee, G.G. (2006). Amino acid residues in the N-terminal region of the PA subunit of influenza A virus RNA polymerase play a critical role in protein stability, endonuclease activity, cap binding, and virion RNA promoter binding. J. Virol. *80*, 7789–7798.

Hatada, E., and Fukuda, R. (1992). Binding of influenza A virus NS1 protein to dsRNA in vitro. J. Gen. Virol. *73*, 3325–3329.

Hausmann, S., Marq, J.B., Tapparel, C., Kolakofsky, D., and Garcin, D. (2008). RIG-I and dsRNA-induced IFNbeta activation. PLoS ONE *3*, e3965.

Hornung, V., Ellegast, J., Kim, S., Brzózka, K., Jung, A., Kato, H., Poeck, H., Akira, S., Conzelmann, K.K., Schlee, M., et al. (2006). 5′-Triphosphate RNA is the ligand for RIG-I. Science *314*, 994–997.

Isaacs, A., and Lindenmann, J. (1957). Virus interference. I. The interferon. Proc. R Soc. Lond. B Biol. Sci. *147*, 258–267.

Jackson, D.A., Caton, A.J., McCready, S.J., and Cook, P.R. (1982). Influenza virus RNA is synthesized at fixed sites in the nucleus. Nature *296*, 366–368.

Kato, H., Takeuchi, O., Sato, S., Yoneyama, M., Yamamoto, M., Matsui, K., Uematsu, S., Jung, A., Kawai, T., Ishii, K.J., et al. (2006). Differential roles of MDA5 and RIG-I helicases in the recognition of RNA viruses. Nature *441*, 101–105.

Kato, H., Takeuchi, O., Mikamo-Satoh, E., Hirai, R., Kawai, T., Matsushita, K., Hiiragi, A., Dermody, T.S., Fujita, T., and Akira, S. (2008). Length-dependent recognition of double-stranded ribonucleic acids by retinoic acid-inducible gene-I and melanoma differentiation-associated gene 5. J. Exp. Med. *205*, 1601–1610.

Kilbourne, E.D. (2006). Influenza pandemics of the 20th century. Emerg. Infect. Dis. *12*, 9–14.

Knipe, D.M., and Howley, P.M. (2007). Fields' Virology, Fifth Edition (Philadelphia: Lippincott Williams & Wilkins).

Krug, R.M., St Angelo, C., Broni, B., and Shapiro, G. (1987). Transcription and replication of influenza virion RNA in the nucleus of infected cells. Cold Spring Harb. Symp. Quant. Biol. *52*, 353–358.

Kumar, H., Kawai, T., Kato, H., Sato, S., Takahashi, K., Coban, C., Yamamoto, M., Uematsu, S., Ishii, K.J., Takeuchi, O., and Akira, S. (2006). Essential role of IPS-1 in innate immune responses against RNA viruses. J. Exp. Med. *203*, 1795–1803.

Maines, T.R., Szretter, K.J., Perrone, L., Belser, J.A., Bright, R.A., Zeng, H., Tumpey, T.M., and Katz, J.M. (2008). Pathogenesis of emerging avian influenza viruses in mammals and the host innate immune response. Immunol. Rev. *225*, 68–84.

Malathi, K., Dong, B., Gale, M., Jr., and Silverman, R.H. (2007). Small self-RNA generated by RNase L amplifies antiviral innate immunity. Nature *448*, 816–819.

Marques, J.T., Devosse, T., Wang, D., Zamanian-Daryoush, M., Serbinowski, P., Hartmann, R., Fujita, T., Behlke, M.A., and Williams, B.R. (2006). A structural basis for discriminating between self and nonself double-stranded RNAs in mammalian cells. Nat. Biotechnol. *24*, 559–565.

Mibayashi, M., Martínez-Sobrido, L., Loo, Y.M., Cárdenas, W.B., Gale, M., Jr., and García-Sastre, A. (2007). Inhibition of retinoic acid-inducible gene I-mediated induction of beta interferon by the NS1 protein of influenza A virus. J. Virol. *81*, 514–524.

Myong, S., Cui, S., Cornish, P.V., Kirchhofer, A., Gack, M.U., Jung, J.U., Hopfner, K.P., and Ha, T. (2009). Cytosolic viral sensor RIG-I is a 5′-triphosphate-dependent translocase on double-stranded RNA. Science *323*, 1070–1074.

Opitz, B., Rejaibi, A., Dauber, B., Eckhard, J., Vinzing, M., Schmeck, B., Hippenstiel, S., Suttorp, N., and Wolff, T. (2007). IFNbeta induction by influenza A virus is mediated by RIG-I which is regulated by the viral NS1 protein. Cell. Microbiol. *9*, 930–938.

Pichlmair, A., and Reis e Sousa, C. (2007). Innate recognition of viruses. Immunity *27*, 370–383.

Pichlmair, A., Schulz, O., Tan, C.P., Näslund, T.I., Liljeström, P., Weber, F., and Reis e Sousa, C. (2006). RIG-I-mediated antiviral responses to single-stranded RNA bearing 5′-phosphates. Science *314*, 997–1001.

Pichlmair, A., Schulz, O., Tan, C.P., Rehwinkel, J., Kato, H., Takeuchi, O., Akira, S., Way, M., Schiavo, G., and Reis e Sousa, C. (2009). Activation of MDA5 requires higher-order RNA structures generated during virus infection. J. Virol. *83*, 10761–10769.

Pleschka, S., Jaskunas, R., Engelhardt, O.G., Zürcher, T., Palese, P., and García-Sastre, A. (1996). A plasmid-based reverse genetics system for influenza A virus. J. Virol. *70*, 4188–4192.

Plumet, S., Herschke, F., Bourhis, J.M., Valentin, H., Longhi, S., and Gerlier, D. (2007). Cytosolic 5′-triphosphate ended viral leader transcript of measles virus as activator of the RIG I-mediated interferon response. PLoS ONE *2*, e279.

Ranjith-Kumar, C.T., Murali, A., Dong, W., Srisathiyanarayanan, D., Vaughan, R., Ortiz-Alacantara, J., Bhardwaj, K., Li, X., Li, P., and Kao, C.C. (2009). Agonist and antagonist recognition by RIG-I, a cytoplasmic innate immunity receptor. J. Biol. Chem. *284*, 1155–1165.

Robb, N.C., Smith, M., Vreede, F.T., and Fodor, E. (2009). NS2/NEP protein regulates transcription and replication of the influenza virus RNA genome. J. Gen. Virol. *90*, 1398–1407.

Saito, T., Owen, D.M., Jiang, F., Marcotrigiano, J., and Gale, M., Jr. (2008). Innate immunity induced by composition-dependent RIG-I recognition of hepatitis C virus RNA. Nature *454*, 523–527.

Samanta, M., Iwakiri, D., Kanda, T., Imaizumi, T., and Takada, K. (2006). EB virus-encoded RNAs are recognized by RIG-I and activate signaling to induce type I IFN. EMBO J. *25*, 4207–4214.

Samuel, C.E. (2001). Antiviral actions of interferons. Clin. Microbiol. Rev. *14*, 778–809.

Schlee, M., Hartmann, E., Coch, C., Wimmenauer, V., Janke, M., Barchet, W., and Hartmann, G. (2009a). Approaching the RNA ligand for RIG-I? Immunol. Rev. *227*, 66–74.

Schlee, M., Roth, A., Hornung, V., Hagmann, C.A., Wimmenauer, V., Barchet, W., Coch, C., Janke, M., Mihailovic, A., Wardle, G., et al. (2009b). Recognition of 5′ triphosphate by RIG-I helicase requires short blunt double-stranded RNA as contained in panhandle of negative-strand virus. Immunity *31*, 25–34.

Schmidt, A., Schwerd, T., Hamm, W., Hellmuth, J.C., Cui, S., Wenzel, M., Hoffmann, F.S., Michallet, M.C., Besch, R., Hopfner, K.P., et al. (2009). 5′-triphosphate RNA requires base-paired structures to activate antiviral signaling via RIG-I. Proc. Natl. Acad. Sci. USA *106*, 12067–12072.

Takahasi, K., Yoneyama, M., Nishihori, T., Hirai, R., Kumeta, H., Narita, R., Gale, M., Jr., Inagaki, F., and Fujita, T. (2008). Nonself RNA-sensing mechanism of RIG-I helicase and activation of antiviral immune responses. Mol. Cell *29*, 428–440.

Tiley, L.S., Hagen, M., Matthews, J.T., and Krystal, M. (1994). Sequence-specific binding of the influenza virus RNA polymerase to sequences located at the 5′ ends of the viral RNAs. J. Virol. *68*, 5108–5116.

Uzri, D., and Gehrke, L. (2009). Nucleotide sequences and modifications that determine RIG-I/RNA binding and signaling activities. J. Virol. *83*, 4174–4184.

Wang, X., Li, M., Zheng, H., Muster, T., Palese, P., Beg, A.A., and García-Sastre, A. (2000). Influenza A virus NS1 protein prevents activation of NF-kappaB and induction of alpha/beta interferon. J. Virol. *74*, 11566–11573.

Wreschner, D.H., McCauley, J.W., Skehel, J.J., and Kerr, I.M. (1981). Interferon action—sequence specificity of the ppp(A2′p)nA-dependent ribonuclease. Nature *289*, 414–417.

Yoneyama, M., and Fujita, T. (2009). RNA recognition and signal transduction by RIG-I-like receptors. Immunol. Rev. *227*, 54–65.

Preference of RIG-I for short viral RNA molecules in infected cells revealed by next-generation sequencing

Alina Baum[a], Ravi Sachidanandam[b], and Adolfo García-Sastre[a,c,d,1]

[a]Department of Microbiology, [c]Division of Infectious Diseases, Department of Medicine, [d]Global Health and Emerging Pathogens Institute, and [b]Department of Genetics and Genomic Sciences, Mount Sinai School of Medicine, New York, NY 10029

Edited by Francis V. Chisari, The Scripps Research Institute, La Jolla, CA, and approved August 10, 2010 (received for review April 14, 2010)

Intracellular detection of virus infections is a critical component of innate immunity carried out by molecules known as pathogen recognition receptors (PRRs). Activation of PRRs by their respective pathogen-associated molecular patterns (PAMPs) leads to production of proinflamatory cytokines, including type I IFN, and the establishment of an antiviral state in the host. Out of all PRRs found to date, retinoic acid inducible gene I (RIG-I) has been shown to play a key role in recognition of RNA viruses. On the basis of in vitro and transfection studies, 5′ppp RNA produced during virus replication is thought to bind and activate this important sensor. However, the nature of RNA molecules that interact with endogenous RIG-I during the course of viral infection has not been determined. In this work we use next-generation RNA sequencing to show that RIG-I preferentially associates with shorter, 5′ppp containing viral RNA molecules in infected cells. We found that during Sendai infection RIG-I specifically bound the genome of the defective interfering (DI) particle and did not bind the full-length virus genome or any other viral RNAs. In influenza-infected cells RIG-I preferentially associated with shorter genomic segments as well as subgenomic DI particles. Our analysis for the first time identifies RIG-I PAMPs under natural infection conditions and implies that full-length genomes of single segmented RNA virus families are not bound by RIG-I during infection.

Sendai | influenza | interferon | pathogen-associated molecular pattern | defective-interfering particle

The retinoic acid inducible gene I (RIG-I)–like receptor (RLR) family of viral sensors contains three members that include the retinoic acid inducible gene (RIG-I), melanoma differentiation factor 5 (MDA5), and Laboratory of Genetics and Physiology gene 2 (LGP2) (1–4). Both RIG-I and MDA5 have been shown to play an important role in recognition of RNA viruses. For most RNA viruses both receptors contribute to IFN induction, although the relative contribution may be cell type specific (5–7). Some viruses, such as picornaviruses and influenza virus, appear to be recognized by only one of the sensors, with picornaviruses being sensed by MDA5 and influenza viruses by RIG-I (1, 8, 9). The substrate specificities of RIG-I and MDA5 have not been clearly established, although from RNA transfection experiments in knockout cells it appears that RIG-I recognizes RNA of various lengths with 5′-triphosphates and some partial double-stranded characteristics, whereas MDA5 senses only very long dsRNA molecules (>2,000 nt) in a phosphate-independent manner (10–14). All RLRs are members of the DExD/H family of RNA helicases and contain an ATP-dependent helicase domain and a C-terminal regulatory domain (RD). The N termini of RIG-I and MDA5 contain two tandem CARD domains required for downstream signaling through their adaptor, MAVS (15–18). The RD domain of RIG-I is responsible for recognition and binding to its RNA substrates in a 5′-phosphate–dependent manner, whereas the helicase domain has affinity for dsRNA (19–21). In uninfected cells RIG-I is thought to exist in an inactive state; the C-terminal RD domain is proposed to interact with the N-terminal CARD domain and block it from association with MAVS. RNA binding to the RD of RIG-I likely induces a conformational change in the protein, resulting in CARD exposure and association with the CARD domain of MAVS.

Because both RIG-I and MDA5 are localized in the cytoplasm, it is imperative for these receptors to be able to distinguish self RNA from viral RNA to prevent IFN production in the absence of infection. The characteristics of RNA molecules capable of activating RIG-I have been well established through numerous biochemical and knockout studies. The signature features of RIG-I agonists are a 5′-triphosphate group at the end of an RNA molecule longer than at least 19 nt and some dsRNA regions (10, 11). Additionally, 5′ppp containing RNAs rich in U residues have been found to act as more potent inducers of RIG-I, indicating that sequence composition might play a role in activation (22). It is yet unclear whether ssRNA, even in the presence of a 5′-triphosphate group, is capable of inducing RIG-I activity, and at least in the case of shorter RNA molecules it appears that some double-stranded characteristics are required for its activation (12, 13).

Although RNA molecules capable of inducing RIG-I have been well characterized, it remains to be seen which if any of these RNAs are actually interacting with RIG-I in virus-infected cells. A recent study using overexpressed RIG-I has shown that this protein associates with negative stranded viral RNA in Sendai virus-infected (SeV) cells and concluded that genomic RNA serves as a inducer of RIG-I signaling (3). In our study we examine SeV-infected cells and analyze RNA molecules that interact with endogenous RIG-I protein both early and late in viral infection. By applying deep sequencing analysis to examine the isolated RNA species we were able to identify the exact nature of RIG-I–associated viral RNA in an unbiased manner. Through this approach we determined that in SeV-infected cells, RIG-I specifically associates with the defective interfering RNA genomes and not with the full-length genomes, mRNA, and leader or trailer RNAs. The immunostimulatory effects of RIG-I–associated RNA in SeV-infected cells were abolished upon removal of all three or two 5′-terminal phosphates. In influenza PR8 ΔNS1 virus-infected cells we observed that RIG-I associates with all genomic segments, but preferentially associates with shorter RNA molecules, such as the NS and M segments, and the internal deletion defective interfering (DI) particles generated by PB1 and PA segments. On the basis of our work we conclude that under natural infection conditions RIG-I preferentially associates with shorter viral RNAs that contain 5′ triphosphates and some dsRNA regions. This study represents a unique analysis of endogenous RIG-I/pathogen-associated molecular pattern (PAMP) complexes present during viral infections.

Author contributions: A.B. and A.G.-S. designed research; A.B. performed research; R.S. contributed new reagents/analytic tools; A.B. and A.G.-S. analyzed data; and A.B. and A.G.-S. wrote the paper.

The authors declare no conflict of interest.

This article is a PNAS Direct Submission.

Freely available online through the PNAS open access option.

[1]To whom correspondence should be addressed. E-mail: adolfo.garcia-sastre@mssm.edu.

This article contains supporting information online at www.pnas.org/lookup/suppl/doi:10.1073/pnas.1005077107/-/DCSupplemental.

Results

Isolation of RIG-I/RNA Complexes from Virus-Infected Cells. To analyze endogenous RNA substrates of RIG-I, A549 human lung carcinoma cells were infected with Sendai virus Cantel (Sev-C) at a high multiplicity of infection (MOI) and infection was allowed to proceed for 24 h. At this time the cells were lysed and RIG-I/RNA complexes were immunoprecipitated with a monoclonal antibody against RIG-I. Fig. 1*A* outlines the overall schematic for the experimental procedure. To make sure that we could distinguish between RIG-I–associated RNA and RNA precipitated in a nonspecific way, an anti-GFP antibody was used in parallel. As can be seen from Fig. 1*B*, precipitation of endogenous RIG-I was very efficient and the vast majority of RIG-I protein was isolated from cell lysates. Following immunoprecipitation (IP), coimmunoprecipitated RNA was isolated by phenol/chlorophorm extraction and transfected into a 293T ISRE-FF (containing a firefly luciferase gene under the control of an IFN-stimulated promoter) reporter cell line to analyze the immunostimulatory activity of the isolated RNA species. Transfection of RIG-I–associated RNA into the reporter cells resulted in a 90-fold increase in reporter activity compared with the GFP control, indicating that the immunostimulatory RNA was specifically pulled down in association with RIG-I (Fig. 1*C*). Comparison of ISRE-FF activity between RIG-I–associated RNA and decreasing amounts of total RNA from SeV-C–infected A549 cells revealed that RIG-I immunoprecipitation greatly concentrates the immunostimulatory activity of the RNA generated in virus-infected cells, demonstrating that RIG-I pulldown is specifically enriching for immunogenic RNA (Fig. 1*D*).

Biochemical Analysis of RIG-I–Associated RNA from SeV-C–Infected Cells. Previous studies have shown that multiple types of RNA molecules are capable of activating RIG-I. These RNAs have been described to contain 5′-triphosphates, diphosphates and monophosphates, and 3′-monophosphates; to be either single- or double-stranded; and to span the length from 19 to thousands of nucleotides long (3, 10–14, 20, 21, 23–25). Enzymatic analysis of immunoprecipitated RNA bound to RIG-I allowed us to characterize the biochemical nature of endogenous RIG-I inducers in SeV-infected cells. Treatment of isolated RNA with RNAseA led to complete loss of immunostimulatory activity in both RIG-I–associated RNA and control RNA, confirming that the PAMPs associated with RIG-I in SeV-infected cells are indeed RNA molecules (Fig. 2*A*). To address the phosphate composition of RIG-I–associated RNA we treated the isolated RNA with calf alkaline phosphatase (CIP), an enzyme that removes all 5′ and 3′ phosphates. Treatment of RIG-I IP RNA with CIP resulted in complete loss of its immunostimulatory activity similarly to control influenza virus genomic RNA, and in contrast to poly(I:C), a synthetic dsRNA molecule with a 5′ monophosphate that does not rely on phosphate composition for its immunostimulatory activity (Fig. 2*B*). Treatment of RIG-I–associated RNA with tobacco acid pyrophosphotase (TAP), which removes the first two terminal phosphates and leaves on a monophosphate group, also led to a complete loss of immunostimulatory activity, demonstrating that RNA species associated with RIG-I during SeV infection require an intact 5′ triphosphate for immogenicity (Fig. 2*C*).

Deep Sequencing of RIG-I–Associated RNA from SeV-C–Infected Cells. To identify the exact nature of RIG-I–associated RNA in an unbiased manner, deep sequencing analysis was performed on the isolated RNA species. The RNA was prepared for sequencing according to Illumina mRNA-seq protocol and sequenced on the Illumina Genome Analyzer. The Illumina platform provides deep coverage, on the order of 10–25 million reads per sequencing sample with relatively short length reads of 29 nt. On the basis of sample preparation methodology both negative and positive sense RNAs are amplified in an identical way and the two forms cannot be distinguished when mapped to their genomic location. Sequences were mapped to the SeV genome and relative abundances of these sequences between RIG-I pulldown and GFP control pulldown, as well as total RNA from SeV-infected cells, were compared. Fig. 3*A* shows the graphical representation of sequences mapped to the SeV genome. Individual peaks on the graph correspond to a sequencing read that starts at that particular position and extends in either direction. The *x* axis corresponds to all possible 15,384 positions in the SeV genome, and the

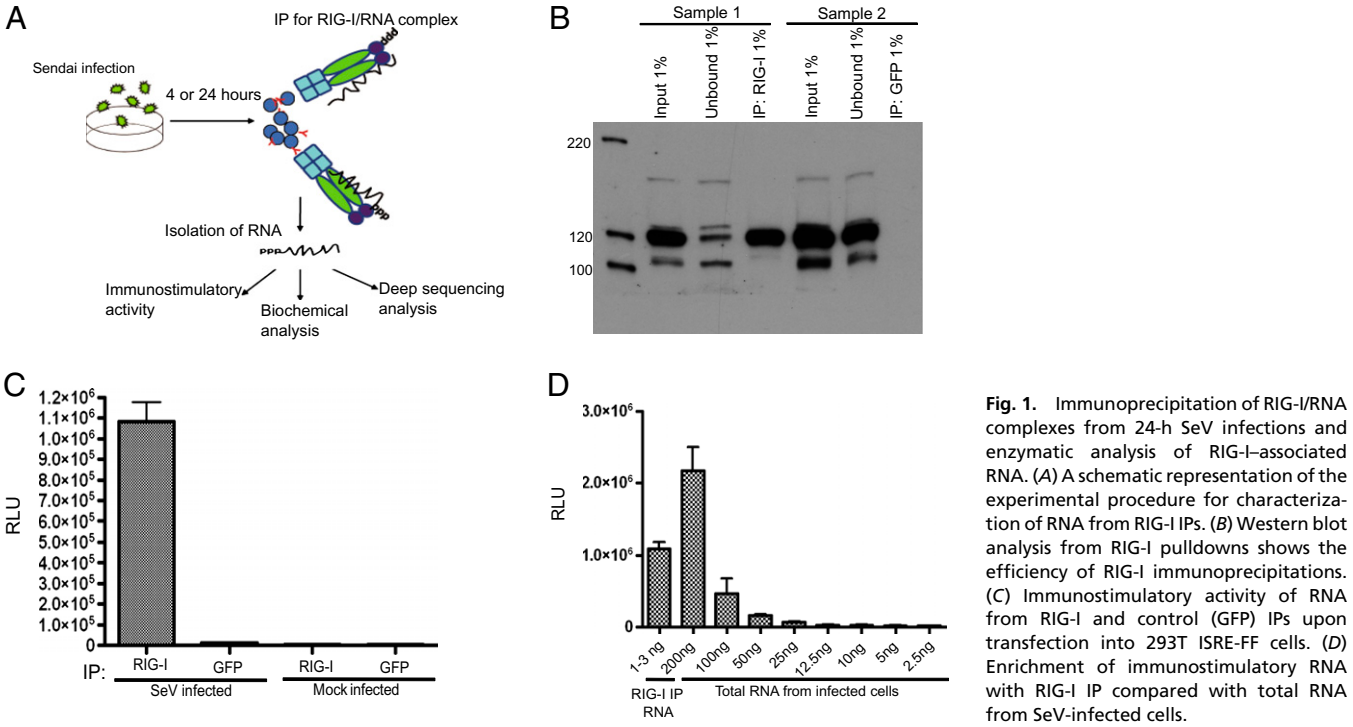

Fig. 1. Immunoprecipitation of RIG-I/RNA complexes from 24-h SeV infections and enzymatic analysis of RIG-I–associated RNA. (*A*) A schematic representation of the experimental procedure for characterization of RNA from RIG-I IPs. (*B*) Western blot analysis from RIG-I pulldowns shows the efficiency of RIG-I immunoprecipitations. (*C*) Immunostimulatory activity of RNA from RIG-I and control (GFP) IPs upon transfection into 293T ISRE-FF cells. (*D*) Enrichment of immunostimulatory RNA with RIG-I IP compared with total RNA from SeV-infected cells.

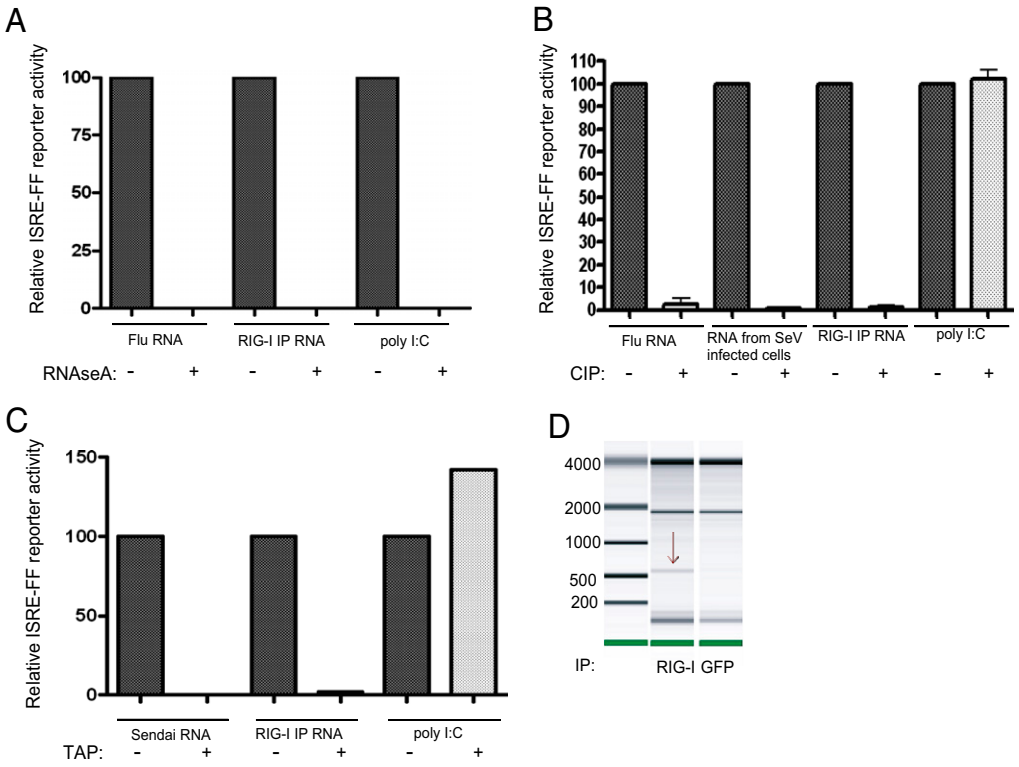

Fig. 2. (*A*) RNAseA treatment of RIG-I bound RNA as well as the control RNAs completely abolishes their immunostimulatory activity. (*B*) CIP treatment of RIG-I bound RNA as well as flu RNA and RNA from SeV-infected cells but not poly (I:C) leads to loss of all immunostimulatory activity. (*C*) TAP treatment of RIG-I bound RNA and purified SeV virus RNA unlike poly(I:C) leads to a complete loss in immunostimulatory activity. (*D*) Agilent mRNA chip of RIG-I–associated RNA reveals a distinct 550-nt band not present in the control IP.

y axis shows the number of reads that begin at that position. Analysis of obtained reads revealed significant variations in peak intensities between close positions on the genome; this variation is clearly observed in Fig. 3*B*. These peaks were similarly distributed between the RIG-I IP sample and the GFP IP sample, indicating to us that they were most likely due to sequencing biases and not to real differences in RNA abundances that could be due to cellular processing of viral RNA. To make sure that this is the case we sequenced viral RNA isolated from purified Sendai virus. Analysis of peak distributions across the same region of the genome (i.e., positions 14,900 and 15,384) revealed that the same nucleotide positions were overrepresented in the purified virus RNA as in our IP samples. On the basis of this evidence we conclude that the variation in peak intensities observed between adjacent genomic positions is due to sequencing biases introduced by the Illumina platform. Examination of SeV sequences from total cellular RNA clearly illustrated that the vast majority of viral RNA mapped to the 5′ end of the SeV genome [Fig. 3*A* (teal color) and Fig. S1]. Specifically, RNA mapping to a region of the genome between positions 14,932 and 15,384 was much more abundant in infected cells than RNA mapping to the rest of the SeV genome. Because it is known from previous studies that the SeV-C copy-back DI particle genome maps to precisely those positions, we concluded that the majority (≈95%) of viral RNA species present in infected cells at 24 h postinfection (hpi) are of a copy-back DI nature (26). Comparison of RIG-I–associated RNA with that of the control IP revealed that the RIG-I pulldown was specifically enriched in DI RNA, with RIG-I samples containing approximately seven times more DI RNA than control samples (Fig. 3 *A*–*C*). None of the other SeV RNAs, including genomic RNA, mRNAs, and leader or trailer were overrepresented in the RIG-I pulldown (Fig. 3*A Lower*). SeV DI copy-back genomes consist of the SeV trailer sequence at the 5′ end, followed by the partial sequence of the L gene and a sequence that is the exact complement to the trailer (antitrailer) at the 3′ end of the molecule (Fig. 3*B*). This unique DI genome structure results in a 546-nt RNA molecule with a relatively long perfect dsRNA portion (92 nt) (very different from typical RNA virus genomes, which contain only short regions of perfect dsRNA). Visualization of a 550-nt band on the Agilent bioanalyzer RNA chip in the RIG-I IP sample but not in the control IP supports the conclusion that the DI genome is preferentially interacting with RIG-I (Fig. 2*D*). Identification of copy-back DIs as a RIG-I PAMP agrees with previous characterization of these molecules as exceptionally good inducers of the IFN response (26).

Analysis of RIG-I–Associated RNA at Early Times of SeV Infection. We next determined whether the same or different viral RNA species are associated with RIG-I relatively early in infection. We followed the same approach as described for the 24 h infection with the exception of lysing cells 4 h postinfection. As can be seen from Fig. S2*A*, we were able to isolate immunostimulatory RNA in a RIG-I–specific manner from these cells, and this RNA was again subjected to deep sequencing analysis. The relative amount of DI genomes in these cells was lower than at the 24-h time point with ≈34% of SeV RNA molecules mapping to the DI genome. Despite DI's lower abundance in these cells it was again found to be the only Sendai RNA that was specifically associating with RIG-I and we did not see any RIG-I–specific binding of the full-length genome (Fig. S2 *B* and *C*). Therefore it appears that RIG-I interacts with the same SeV-derived RNA molecule both early and late in infection, namely DI RNA.

Confirmation of Deep Sequencing Data with Quantitative PCR. To validate our deep sequencing analysis with an independent method we chose to perform TaqMan Q-PCR RNA quantification. On the basis of the unique structure of the SeV copy-back DI, with the 3′ end of the molecule containing an antitrailer (Fig. 3*B*), it is possible to design PCR primers that will detect only the DI RNA and not the full-length genome, L mRNA, or trailer RNA. Comparison of relative abundances of DI RNA and genome RNA/L mRNA between total RNA from infected cells, RIG-I IP and GFP IP at 24 hpi confirmed that only DI-specific

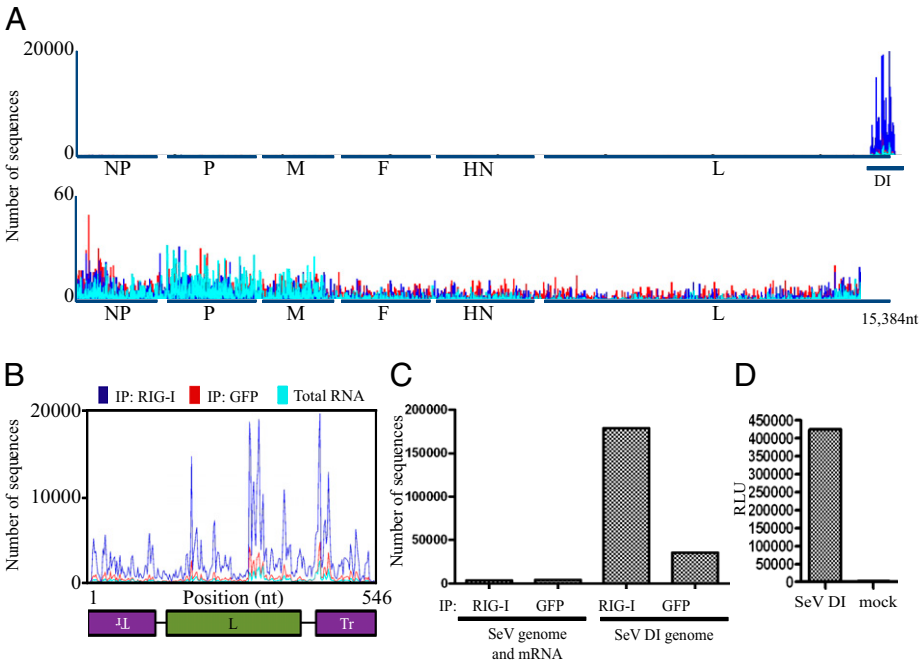

Fig. 3. Deep sequencing analysis of RIG-I–associated and control IP RNA from SeV virus-infected cells. (*A*) RNA from RIG-I IP and control (GFP) IP and total RNA from SeV-infected cells (blue, red, and teal, respectively) were subjected to Illumina deep sequencing. Obtained sequencing reads are mapped to their starting position on the virus genome; the *y* axis shows the number of sequences mapped to a particular position. (*Upper*) All sequences mapped to the entire genome are shown. (*Lower*) The last 484 nt are removed to allow better visualization of the rest of the genome (note the difference in the *y* scale between *Upper* and *Lower*). (*B*) Sequencing reads mapped to the genome of the DI particle show enrichment for RIG-I–associated sequences throughout the entire DI molecule. (*C*) Comparison of numbers of sequences that map to the DI genome or the rest of the SeV genome in the RIG-I and control (GFP) IPs. (*D*) Induction of ISRE-FF reporter by transfection of T7 SeV DI RNA compared with mock transfected cells.

sequences were enriched in RIG-I IPs (Fig. S3*A*), validating conclusions from our deep sequencing data. To obtain sense-specific information about ratios of DI genome to full-length genome (excluding L mRNA sequences) we performed the same Q-PCR analysis except with sense-specific RT amplification. Again we saw that only DI genomic RNA and not the full-length genome was preferentially interacting with RIG-I (Fig. S3*C*). We also attempted to analyze RIG-I–associated RNA very early on in SeV-infected cells by allowing the infection to progress for only 30 min or 1 h. Immunoprecipitation of RIG-I at these early time points did not produce any immunostimulatory RNA (Fig. S3*B*) nor could we detect any significant differences in either full-length genome or DI genome abundance in RIG-I–associated RNA (Fig. S3*C*). This failure to detect immunostimulatory RNA very early in infection could possibly be due to limited sensitivity of our methodology or requirement for higher levels of virus replication to induce the antiviral response.

Isolation and Deep Sequencing of RIG-I–Associated RNA from Influenza PR8ΔNS1 Virus Infections. We next attempted to characterize RNA molecules associated with RIG-I during influenza virus infection, as it possesses a very different genome organization and replication cycle compared with Sendai virus. Because wild-type influenza virus is very efficient at blocking IFN induction through the action of its well-characterized IFN antagonist NS1 (27), we decided to infect A549 cells with PR8ΔNS1 virus. This mutant virus is lacking the RNA sequence that codes for the NS1 protein and therefore it is unable to block IFN production and RIG-I up-regulation in infected cells. Isolation of RIG-I/RNA complexes from A549 cells infected with a high MOI of PR8ΔNS1 virus produced RNA that was specifically immunostimulatory upon transfection into the 293T ISRE-FF reporter cell line compared with the RNA isolated from the control anti-GFP pulldown (Fig. 4*B*). Again to identify which viral RNA species were specifically interacting with RIG-I in infected cells we performed deep sequencing analysis of all isolated RNA. The obtained sequences were mapped to the influenza virus PR8 genomes and analyzed for abundances between the RIG-I IP sample and the control IP sample. Fig. 4*A* shows the obtained sequencing reads mapped to each segment of the influenza virus genome. For all genomic segments we saw a higher abundance of RNA in RIG-I IP samples than in the control samples, with the average ratio between RIG-I IP and control of 2.6. To establish that this difference represents a significant change in abundance between the two samples we compared the relative abundances of eight randomly picked cellular mRNAs from the same sequencing dataset. The average ratio between RIG-I IP and the control IP for these eight mRNAs was 1.1 (Table S1). Therefore, we conclude that we have identified RNAs that specifically interact with RIG-I in the course of influenza virus infection.

To see whether specific regions within the individual genome segments were more enriched in the RIG-I pulldown we calculated the RIG-I IP/control IP ratio at each nucleotide position on each segment. These ratios were then averaged over 100-nt intervals and allowed us to visualize the relative enrichment ratios over the length of each genomic segment (Fig. 5). This analysis revealed that the 5′ and 3′ regions in the PB1 and PA segments were more overrepresented in RIG-I pulldowns than the rest of those segments. We hypothesized that these regions might represent internal deletion DI particles that have previously been shown to be associated with influenza virus replication (28). RT-PCR of the PA gene with primers corresponding to the ends of the segment indeed produced a 650-nt product that was not observed in the same RT-PCR performed with purified RNA from PR8 influenza virus virions; this RNA was sequenced and confirmed to map to the ends of the PA segment. Comparison of RIG-I IP/control IP RNA ratios between the segments identifies the two DI RNAs from PA and PB1 segments as well as the NS and M segments as being the most enriched RNA molecules in the RIG-I pulldown (Fig. 5). On the basis of these observations we propose that RIG-I binds to all segments of the flu genome but preferentially associates with shorter RNA molecules such as the shorter influenza virus segments and short DI particles generated from the larger segments.

Immunostimulatory Activity of Individual PR8 RNA Genomic Segments. To check that RIG-I–associated viral RNA molecules identified in our pulldowns could act as PAMPs and induce an antiviral response, we generated six of these RNAs by T7 promoter-driven in vitro transcription. The size and purity of

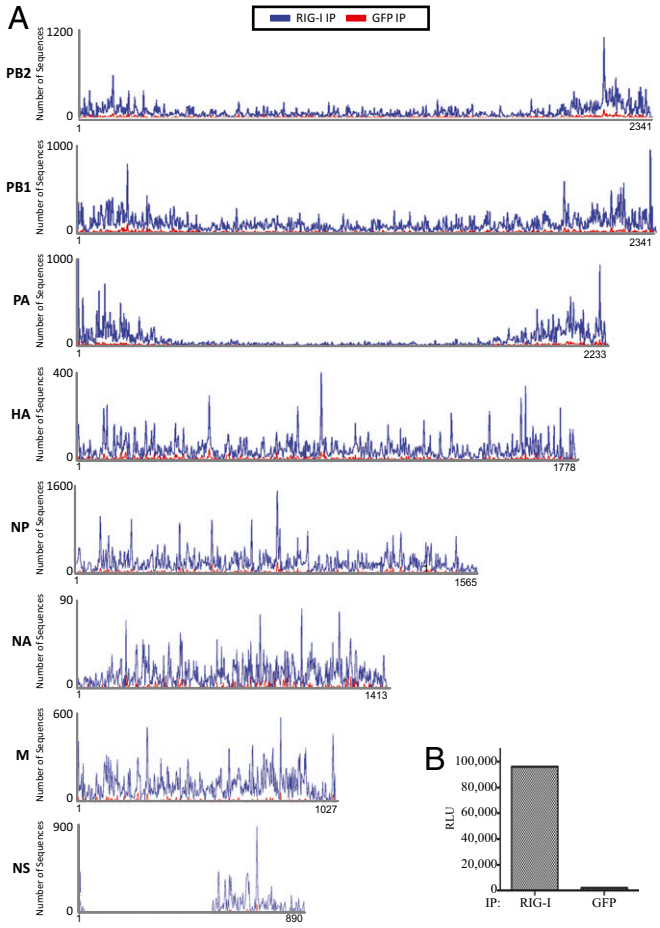

Fig. 4. Immunoprecipitation and deep sequencing analysis of RIG-I–associated RNA from 24-h influenza virus infections. (*A*) Sequencing reads from RIG-I and control (GFP) IPs were mapped to the individual PR8 influenza virus genomic segments. Each peak corresponds to the beginning position of that particular read and the number of sequences starting at that position is represented on the *y* axis. RIG-I enrichment (blue) can be observed on all genomic segments. (*B*) Transfection of RIG-I–associated RNA into the ISRE-FF reporter cells shows high immunostimulatory activity of this RNA compared with the control (GFP) IP.

produced RNAs were checked by denaturing agarose gel electrophoresis (Fig. S4*A*). Transfection of equimolar ratios of these RNAs into the ISRE-FF reporter cells resulted in induction of the FF reporter, indicating that all of these RNAs were indeed immunogenic (Fig. S4*B*). With the exception of NA RNA, which gave the lowest amount of induction, we did not see any significant differences in reporter stimulation between the different flu RNAs, and thus immunogenicity of these RNAs was not proportional to RNA length. Currently we do not understand the molecular basis or significance of the observed differences in RIG-I association between various influenza RNAs. These differences could potentially reflect variability in RNA segment accessibility to RIG-I during the course of infection, either structurally or spatially. Also, because T7 transcribed RNAs are naked RNAs transfected into cells, their localization, stability, and interactions with RIG-I might be fundamentally different from those that take place during viral infection.

Discussion

By subjecting the RNA to both biochemical and deep sequencing analysis we have been able to pinpoint the exact nature of RNA molecules that interact with RIG-I during the course of SeV and influenza virus infections and induce the antiviral response through the RIG-I signaling pathway. The application of deep sequencing techniques allowed us to examine the RNA molecules without any a priori assumptions about their identity and eliminated biases commonly introduced by more traditional methods such as Northerns and quantitative PCR where the selection of primers and probes can greatly influence the observed result. We conclude that viral replicating RNA constitutes the majority of the viral immunostimulatory RNA associated with RIG-I. In infections with both viruses we observed that shorter molecules preferentially associate with RIG-I over longer ones even though all of these RNAs should contain identical 5′-triphosphorylated ends. The preference of RIG-I for shorter substrates might explain why influenza virus has been shown to be exclusively recognized by RIG-I unlike most other RNA viruses that normally rely on both RIG-I and MDA5 recognition. All of the molecules we have identified as specifically interacting with RIG-I also contain some dsRNA regions directly adjacent to the triphosphate, supporting conclusions from previous work that this panhandle-type architecture of the RNA molecule may be preferentially recognized by RIG-I (12, 13). The identification of the influenza virus NS segment and SeV DI RNA as preferred substrates of RIG-I also agrees with their predicted roles as RIG-I PAMPs on the basis of the U-rich composition of this RNA (22). It will be very interesting to see what types of RNAs associate with RIG-I in infections with other viruses and whether generation of DI particles by *Mononegavirales* members is a prerequisite for RIG-I activation. The extent of secondary structure characteristics in viral RNA would be expected to vary highly between various viruses and the exact role these differences might play in RIG-I activation is an interesting and complex question. The fact that CIP and TAP treatment led to complete loss of DI's ability to induce an immunostimulatory response is interesting and illustrates that the 5′ triphosphate (although a diphosphate has not been experimentally ruled out in this study) is required even in the context of a relatively long dsRNA region, such as SeV DI RNA. Our finding that DI subgenomic

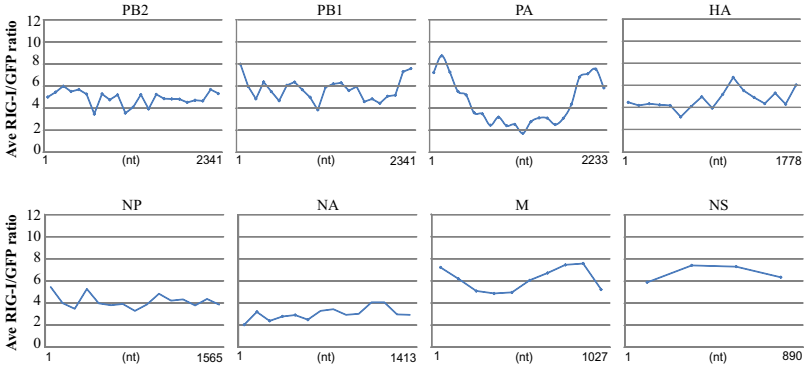

Fig. 5. Analysis of average local enrichment of influenza virus RNA in RIG-I versus control (GFP) immunoprecipitations. For each genomic segment ratios of RIG-I/GFP sequencing reads were calculated at each nucleotide position. The average of these ratios for every 100 nt was calculated and is shown.

particles preferentially associate with RIG-I provides an explanation for the historical observation that viruses containing these particles act as superior IFN inducers (26, 29). The approach we used in our work provides a powerful tool for analysis of RIG-I–associated RNA from various viral infections in multiple cell types as well as other protein/RNA complexes.

Materials and Methods

RIG-I/RNA Complex Immunoprecipitation. A549 human lung carcinoma cells were infected with a high MOI of SeV-C or PR8ΔNS1 viruses. Infections were allowed to proceed for 24 or 4 h and the cells were washed five times with cold PBS and lysed in a 0.5% Nonidet P-40 buffer. Lysates were frozen at −80 °C before being subjected to immunoprecipitation with either an anti-RIG-I antibody or an anti-GFP antibody (Abcam ab1218). Fractions from IPs were obtained during the process and frozen for future protein analysis. RNA was isolated from agarose beads by proteinase K treatment in SDS buffer and phenol/chlorophorm extraction followed by ethanol precipitation. Immunostimulatory activity of isolated RNA was analyzed by transfecting a small fraction of RNA into a 293T ISRE-FF reporter cell line and measurement of FF activity.

Biochemical Analysis of RNA. Isolated RNA was subjected to treatment with RNAseA (Qiagen), CIP (Promega), and TAP (Epicentre) and transfected into the 293T ISRE-FF reporter cell line following each treatment to assay potential loss of immunostimulatory activity. As controls, purified influenza PR8 virus RNA, purified SeV-C RNA, total RNA from SeV-C–infected cells, and poly(I:C) were used in various experiments. Viral RNA was isolated from sucrose cushion purified virus with phenol/chlorophorm or TRIzol (Invitrogen) extraction, and total cellular RNA was isolated with TRIzol extraction. Agilent RNA chip analysis was performed at the microarray facility at Mount Sinai School of Medicine using the mRNA chip.

Deep Sequencing Analysis of RNA. Total RNA isolated from immunoprecipitations or from cell lysates was prepared for Illumina sequencing using the mRNA-Seq (Illumina) sample preparation kit according to manufacturer's instruction. To analyze all RNA species present, the initial poly(A) RNA isolation step was omitted. Because ribosomal RNA presented an overwhelming portion of all RNA in either immunoprecipitations or total cellular RNA, a RiboMinus Eukaryote Kit for RNA-Seq (Invitrogen) was used before deep sequencing to remove a large portion of ribosomal species. The RNA was checked following ribosomal RNA removal for its ability to induce the ISRE-FF reporter, thereby excluding the removed ribosomal sequences as possible inducers of RIG-I. Sequencing was performed on the Illumina Genome Analyzer in the Mount Sinai sequencing facility. Obtained sequences were mapped to human and viral genomes and relative abundances were analyzed between RIG-I pulldown and control samples. Average ratios for influenza virus genomic segments between RIG-I pulldown and control pulldowns were calculated by determining the relative sequence abundance at each position on the genomic segment and calculating the average of those ratios over every 100 nt.

TaqMan Quantitative PCR Analysis. Q-PCR analysis was performed with utilization of Roche LightCycler 480 technology. All Q-PCR reactions incorporated multiplexed human actin β internal controls and relative abundance of each RNA was calculated with reference to this control.

T7 RNA Transcription. Templates for T7 RNA transcription were synthesized from PR8 pDZ plasmids coding for individual RNA segments of influenza PR8 virus (30). T7 SeV-C DI particle template was created by RT amplification of SeV DI RNA from infected cells. A truncated T7 promoter was added to each DNA segment by PCR. T7 transcription reactions were carried out with a T7 MEGAscript kit (Ambion). RNA was purified with RNAeasy columns (Qiagen) and analyzed on denaturing agarose gels for correct size and purity.

ACKNOWLEDGMENTS. We thank Dr. Estanislao Nistal-Villan (Mount Sinai School of Medicine, New York, NY) for the RIG-I antibody, Dr. Adam Vigil (University of California, Irvine, CA) for assistance with manuscript preparation, Dr. Luis Martinez-Sorbido (University of Rochester, Rochester, NY) for the 293T ISRE-FF cell line, Richard Cadagan and Osman Lizardo for technical assistance, and Mount Sinai sequencing facility for assistance with deep sequencing processing and analysis. This research was partly funded by National Institutes of Health Grants R01AI46954, U19AI83025, U01AI082970, and U54AI57168 and by the National Institute of Allergy and Infectious Diseases-funded Center for Research in Influenza Pathogenesis (HHSN266200700010C). A.B. is supported by National Institute of Allergy and Infectious Diseases Training Program in Mechanisms of Virus–Host Interactions (2T32AI007647-11).

1. Yoneyama M, et al. (2004) The RNA helicase RIG-I has an essential function in double-stranded RNA-induced innate antiviral responses. *Nat Immunol* 5:730–737.
2. Foy E, et al. (2005) Control of antiviral defenses through hepatitis C virus disruption of retinoic acid-inducible gene-I signaling. *Proc Natl Acad Sci USA* 102:2986–2991.
3. Rehwinkel J, et al. (2010) RIG-I detects viral genomic RNA during negative-strand RNA virus infection. *Cell* 140:397–408.
4. Yoneyama M, et al. (2005) Shared and unique functions of the DExD/H-box helicases RIG-I, MDA5, and LGP2 in antiviral innate immunity. *J Immunol* 175:2851–2858.
5. Yount JS, Gitlin L, Moran TM, López CB (2008) MDA5 participates in the detection of paramyxovirus infection and is essential for the early activation of dendritic cells in response to Sendai virus defective interfering particles. *J Immunol* 180:4910–4918.
6. Melchjorsen J, et al. (2005) Activation of innate defense against a paramyxovirus is mediated by RIG-I and TLR7 and TLR8 in a cell-type-specific manner. *J Virol* 79: 12944–12951.
7. Kato H, et al. (2005) Cell type-specific involvement of RIG-I in antiviral response. *Immunity* 23:19–28.
8. Gitlin L, et al. (2006) Essential role of mda-5 in type I IFN responses to polyriboinosinic: polyribocytidylic acid and encephalomyocarditis picornavirus. *Proc Natl Acad Sci USA* 103:8459–8464.
9. Kato H, et al. (2006) Differential roles of MDA5 and RIG-I helicases in the recognition of RNA viruses. *Nature* 441:101–105.
10. Hornung V, et al. (2006) 5′-Triphosphate RNA is the ligand for RIG-I. *Science* 314: 994–997.
11. Pichlmair A, et al. (2006) RIG-I-mediated antiviral responses to single-stranded RNA bearing 5′-phosphates. *Science* 314:997–1001.
12. Schmidt A, et al. (2009) 5′-triphosphate RNA requires base-paired structures to activate antiviral signaling via RIG-I. *Proc Natl Acad Sci USA* 106:12067–12072.
13. Schlee M, et al. (2009) Recognition of 5′ triphosphate by RIG-I helicase requires short blunt double-stranded RNA as contained in panhandle of negative-strand virus. *Immunity* 31:25–34.
14. Kato H, et al. (2008) Length-dependent recognition of double-stranded ribonucleic acids by retinoic acid-inducible gene-I and melanoma differentiation-associated gene 5. *J Exp Med* 205:1601–1610.
15. Kawai T, et al. (2005) IPS-1, an adaptor triggering RIG-I- and Mda5-mediated type I interferon induction. *Nat Immunol* 6:981–988.
16. Meylan E, et al. (2005) Cardif is an adaptor protein in the RIG-I antiviral pathway and is targeted by hepatitis C virus. *Nature* 437:1167–1172.
17. Seth RB, Sun L, Ea CK, Chen ZJ (2005) Identification and characterization of MAVS, a mitochondrial antiviral signaling protein that activates NF-kappaB and IRF 3. *Cell* 122:669–682.
18. Xu LG, et al. (2005) VISA is an adapter protein required for virus-triggered IFN-beta signaling. *Mol Cell* 19:727–740.
19. Saito T, et al. (2007) Regulation of innate antiviral defenses through a shared repressor domain in RIG-I and LGP2. *Proc Natl Acad Sci USA* 104:582–587.
20. Cui S, et al. (2008) The C-terminal regulatory domain is the RNA 5′-triphosphate sensor of RIG-I. *Mol Cell* 29:169–179.
21. Takahasi K, et al. (2008) Nonself RNA-sensing mechanism of RIG-I helicase and activation of antiviral immune responses. *Mol Cell* 29:428–440.
22. Saito T, Owen DM, Jiang F, Marcotrigiano J, Gale M, Jr (2008) Innate immunity induced by composition-dependent RIG-I recognition of hepatitis C virus RNA. *Nature* 454:523–527.
23. Marques JT, et al. (2006) A structural basis for discriminating between self and nonself double-stranded RNAs in mammalian cells. *Nat Biotechnol* 24:559–565.
24. Malathi K, Dong B, Gale M, Jr, Silverman RH (2007) Small self-RNA generated by RNase L amplifies antiviral innate immunity. *Nature* 448:816–819.
25. Ranjith-Kumar CT, et al. (2009) Agonist and antagonist recognition by RIG-I, a cytoplasmic innate immunity receptor. *J Biol Chem* 284:1155–1165.
26. Strahle L, Garcin D, Kolakofsky D (2006) Sendai virus defective-interfering genomes and the activation of interferon-beta. *Virology* 351:101–111.
27. García-Sastre A, et al. (1998) Influenza A virus lacking the NS1 gene replicates in interferon-deficient systems. *Virology* 252:324–330.
28. Odagiri T, Tashiro M (1997) Segment-specific noncoding sequences of the influenza virus genome RNA are involved in the specific competition between defective interfering RNA and its progenitor RNA segment at the virion assembly step. *J Virol* 71:2138–2145.
29. Marcus PI, Sekellick MJ (1977) Defective interfering particles with covalently linked [+/-]RNA induce interferon. *Nature* 266:815–819.
30. Quinlivan M, et al. (2005) Attenuation of equine influenza viruses through truncations of the NS1 protein. *J Virol* 79:8431–8439.

LETTERS

IκBβ acts to inhibit and activate gene expression during the inflammatory response

Ping Rao[1]†, Mathew S. Hayden[1,2], Meixiao Long[1,2], Martin L. Scott[3]†, A. Philip West[1], Dekai Zhang[1]†, Andrea Oeckinghaus[1,2], Candace Lynch[4], Alexander Hoffmann[4], David Baltimore[3] & Sankar Ghosh[1,2]

The activation of pro-inflammatory gene programs by nuclear factor-κB (NF-κB) is primarily regulated through cytoplasmic sequestration of NF-κB by the inhibitor of κB (IκB) family of proteins[1]. IκBβ, a major isoform of IκB, can sequester NF-κB in the cytoplasm[2], although its biological role remains unclear. Although cells lacking IκBβ have been reported[3,4], *in vivo* studies have been limited and suggested redundancy between IκBα and IκBβ[5]. Like IκBα, IκBβ is also inducibly degraded; however, upon stimulation by lipopolysaccharide (LPS), it is degraded slowly and re-synthesized as a hypophosphorylated form that can be detected in the nucleus[6–11]. The crystal structure of IκBβ bound to p65 suggested this complex might bind DNA[12]. *In vitro*, hypophosphorylated IκBβ can bind DNA with p65 and c-Rel, and the DNA-bound NF-κB:IκBβ complexes are resistant to IκBα, suggesting hypophosphorylated, nuclear IκBβ may prolong the expression of certain genes[9–11]. Here we report that *in vivo* IκBβ serves both to inhibit and facilitate the inflammatory response. IκBβ degradation releases NF-κB dimers which upregulate pro-inflammatory target genes such as tumour necrosis factor-α (TNF-α). Surprisingly, absence of IκBβ results in a dramatic reduction of TNF-α in response to LPS even though activation of NF-κB is normal. The inhibition of TNF-α messenger RNA (mRNA) expression correlates with the absence of nuclear, hypophosphorylated-IκBβ bound to p65:c-Rel heterodimers at a specific κB site on the TNF-α promoter. Therefore IκBβ acts through p65:c-Rel dimers to maintain prolonged expression of TNF-α. As a result, $I\kappa B\beta^{-/-}$ mice are resistant to LPS-induced septic shock and collagen-induced arthritis. Blocking IκBβ might be a promising new strategy for selectively inhibiting the chronic phase of TNF-α production during the inflammatory response.

To understand the biological function of IκBβ better, we studied mice lacking the *IκBβ* gene. Homologous recombination was used to delete most of the IκBβ coding sequences (30–308 amino acids) including elements essential for binding to NF-κB (Supplementary Fig. 2)[6,12,13]. Absence of IκBβ was confirmed by immunoblotting of mouse embryonic fibroblasts (MEFs; Supplementary Fig. 2). Although IκBβ is expressed broadly, including in haematopoietic organs (Supplementary Fig. 3a), the *IκBβ* knockout mice breed and develop normally without any obvious phenotypic defects.

NF-κB and IκB proteins function in an integrated network. Hence reduced expression of one component may cause compensatory changes in levels of other proteins[14,15]. However, expression levels of IκBα, IκBε, p65, RelB, c-Rel, p105 and p100 were unaffected in $I\kappa B\beta^{-/-}$ mice (Supplementary Fig. 3b). Increased NF-κB activity has been observed in other IκB knockouts[16–18], and increased basal NF-κB reporter activity was observed in $I\kappa B\beta^{-/-}$ MEFs (Fig. 1a). Electrophoretic mobility shift assays (EMSAs) demonstrated increased basal NF-κB activity in $I\kappa B\beta^{-/-}$ cells (60%) (Supplementary Fig. 3c). Conversely, overexpression of IκBβ inhibits NF-κB activation (Supplementary Fig. 3d). Thus IκBβ inhibits NF-κB and degradation or loss of IκBβ contributes to NF-κB activity. NF-κB reporter assays reveal that absolute NF-κB activity in response to LPS, IL-1β or TNF-α is slightly higher in the $I\kappa B\beta^{-/-}$ than wild-type cells (Fig. 1a). However, the kinetics of NF-κB activation by EMSA, and the pattern of IκB degradation by immunoblotting, in cells stimulated with LPS, IL-1β or TNF-α were not demonstrably different in $I\kappa B\beta^{-/-}$ cells (Supplementary Fig. 4). Thus, loss of IκBβ results in a modest elevation in basal NF-κB activity, whereas inducible NF-κB activation is relatively unaffected.

NF-κB regulates the expression of many genes, in particular those involved in inflammation and immune responses[19]. To determine whether IκBβ has a role in the inflammatory response, $I\kappa B\beta^{-/-}$ and $I\kappa B\beta^{+/+}$ mice were challenged with LPS. Surprisingly, $I\kappa B\beta^{-/-}$ mice were significantly resistant to the induction of shock (Fig. 1b). We therefore examined the serum levels of the key acute phase cytokines TNF-α, IL-1β and IL-6 (ref. 20) after LPS injection. In wild-type mice TNF-α production peaked 1 h after LPS injection, whereas IL-6 and IL-1β production peaked around 2 h, in agreement with previous studies[21]. Although serum IL-6 and IL-1β were reduced (approximately 25%) in the $I\kappa B\beta^{-/-}$ mice, the reduction of TNF-α levels (greater than 70%) was more striking (Fig. 1c). As the peak of serum TNF-α precedes that of IL-1β and IL-6, it is likely that the reduction of IL-1β and IL-6 is secondary. As monocytes and macrophages are major sources of systemic TNF-α, we analysed LPS-induced cytokines in thioglycollate-elicited peritoneal macrophages (TEPMs). Although equivalent macrophage populations were obtained from the mice (Supplementary Fig. 5a), production of TNF-α, but not IL-6, was drastically reduced in $I\kappa B\beta^{-/-}$ TEPMs (Fig. 1d).

To understand how IκBβ affects TNF-α synthesis we examined each step of TNF-α production. Secreted TNF-α was detectable by enzyme-linked immunosorbent assay (ELISA) after 2 h of LPS stimulation and by 4 h was significantly impaired in $I\kappa B\beta^{-/-}$ TEPMs (Fig. 2a). IL-6 production was equivalent (Fig. 2a). We examined the level of pro-TNF-α by intracellular fluorescence-activated cell sorting and found there was very little pro-TNF-α detected in the $I\kappa B\beta^{-/-}$ TEPMs, even after 8 h of LPS stimulation (Fig. 2b). The average amount of pro-TNF-α produced was two- to threefold higher in wild-type than $I\kappa B\beta^{-/-}$ TEPMs (Fig. 2c). Consistent with this

[1]Department of Immunobiology and Department of Molecular Biophysics & Biochemistry, Yale University School of Medicine, New Haven, Connecticut 06520, USA. [2]Department of Microbiology & Immunology, College of Physicians & Surgeons, Columbia University, New York, New York 10032, USA. [3]Department of Biology, California Institute of Technology, Pasadena, California 91125, USA. [4]Signaling Systems Laboratory, Department of Chemistry and Biochemistry, University of California at San Diego, La Jolla, California 92093, USA. †Present addresses: Department of Molecular Microbiology and Immunology, University of Southern California, Los Angeles, California 90033, USA (P.R.); Merck Research Laboratories, Boston, Massachusetts 02115, USA (M.L.S.); Center for Extracellular Matrix Biology, Texas A & M University Institute of Biosciences and Technology, Houston, Texas 77030, USA (D.Z.).

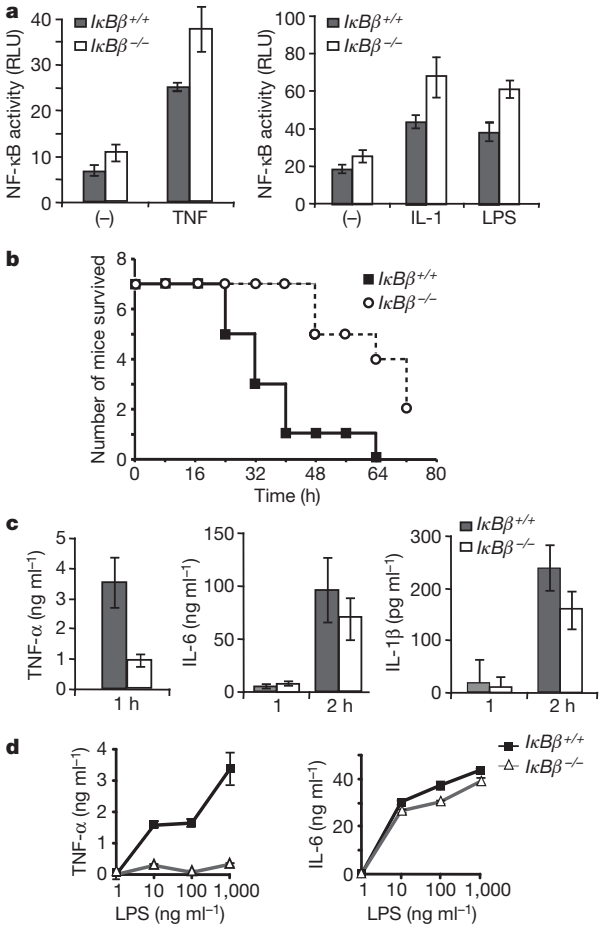

Figure 1 | Mice lacking IκBβ are resistant to LPS-induced endotoxin shock. **a**, Wild-type and $I\kappa B\beta^{-/-}$ MEF cells transfected with pBIIx-luc reporter and *Renilla* luciferase vectors were treated with TNF-α, IL-1β or LPS for 4 h and analysed for luciferase activity. Results are expressed as relative luciferase units (RLU) normalized by *Renilla* luciferase activity; error bars, s.d. ($n = 3$). **b**, Age- and sex-matched mice received intra-peritoneal injection of LPS and survival rates were scored every 8 h for 3 days ($n = 7$). **c**, Serum TNF-α, IL-6 and IL-1β 1 h and/or 2 h after intraperitoneal injection of LPS was examined by ELISA; error bars, s.d. ($n = 5$). **d**, TEPMs from littermate mice were treated for 20 h with LPS as indicated, and TNF-α and IL-6 in the media were determined by ELISA; error bars, s.d. ($n = 3$).

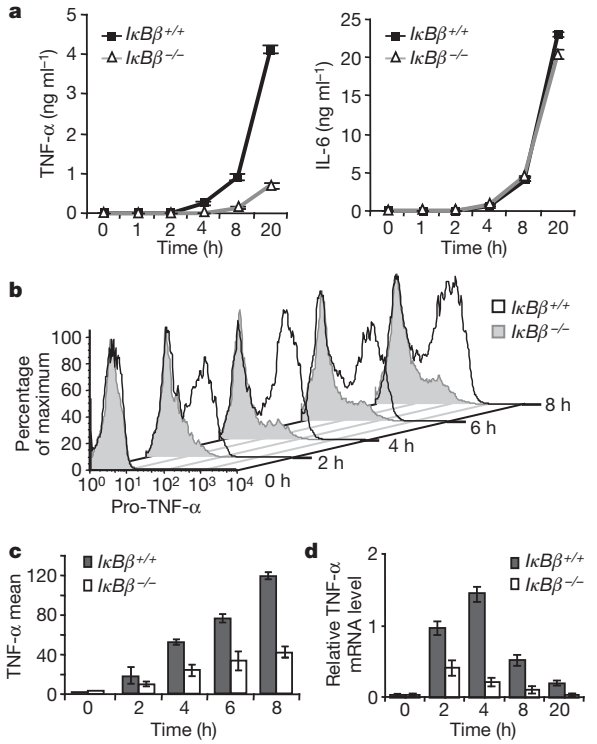

Figure 2 | Deficient TNF-α transcription in $I\kappa B\beta^{-/-}$ macrophages. **a**, TEPMs from littermate wild-type and $I\kappa B\beta^{-/-}$ mice were treated with LPS and secreted TNF-α and IL-6 were determined by ELISA; error bars, s.d. ($n = 3$). **b**, TEPMs from littermate mice were treated as in **a** in the presence of brefeldin A, and intracellular pro-TNF-α was examined with flow cytometry. **c**, Intracellular pro-TNF-α production was examined as in **b** with macrophages isolated from three pairs of littermate mice; error bars, s.d. **d**, TEPMs were stimulated with LPS as in **a** and relative TNF-α mRNA level was determined by qRT–PCR; error bars, s.d. ($n = 3$).

difference in protein levels, steady-state TNF-α mRNA was decreased two- to sixfold in the $I\kappa B\beta^{-/-}$ TEPMs compared with wild-type cells (Fig. 2d). Although TNF-α mRNA is known to be regulated post-transcriptionally[22,23], there was no difference in TNF-α mRNA stability between wild-type and $I\kappa B\beta^{-/-}$ TEPMs (Supplementary Fig. 5b). Therefore, IκBβ promotes TNF-α transcription.

To understand how IκBβ affects TNF-α transcription, we investigated which NF-κB subunits were associated with IκBβ in macrophages. It is known that IκBβ associates with p65:p50 and c-Rel:p50 complexes[24] through direct binding to p65 and c-Rel but not p50 (ref. 6). However, we found that IκBβ could be immunoprecipitated only with p65 and c-Rel, but not p50 (Fig. 3a). Both immunoprecipitations with anti-p65 and anti-c-Rel antibodies pull down IκBβ, IκBα and p50. Thus, there are p65:p50 and inducible c-Rel:p50 complexes that are associated with IκBα or other IκBs, but not IκBβ. Reciprocal immunoprecipitation of p65 with c-Rel and both p65 and c-Rel with IκBβ suggests a p65:c-Rel heterodimer associated with IκBβ (Fig. 3b). To demonstrate the association of IκBβ with p65:c-Rel, we performed sequential immunoprecipitations by first immunoprecipitating IκBβ and then immunoprecipitating the eluted IκBβ complexes with anti-c-Rel antibody. The presence of p65 in the anti-c-Rel immunoprecipitate confirms the presence of an IκBβ:p65:c-Rel complex (Fig. 3c).

The IκBβ:p65:c-Rel complex was found in nuclear extracts, which suggests that this could be a transcriptionally active complex. We had previously reported[10] that IκBβ exists in two phosphorylation states: a hyperphosphorylated state in quiescent, unstimulated cells, and a hypophosphorylated newly synthesized state in LPS-stimulated cells (Supplementary Fig. 6a). In the co-immunoprecipitation experiments shown here we found that both forms of IκBβ can bind p65 and c-Rel, although the hypophosphorylated form predominates in the IκBβ:p65:cRel complex after LPS stimulation.

There are four κB sites upstream of TNF-α coding region, three of which are crucial for NF-κB-dependent TNF-α expression[25]. Therefore, we performed chromatin immunoprecipitation with anti-p65, anti-c-Rel and anti-IκBβ antibodies in RAW264.7 cells and monitored the region encompassing these three κB sites. After LPS stimulation, TNF-α promoter region DNA is enriched by p65, c-Rel and IκBβ antibodies by 56-, 70- and 7-fold respectively (Fig. 3d). In contrast, IκBβ is not recruited to the IL-6 promoter after LPS stimulation whereas p65 and c-Rel are recruited as expected (Fig. 3d). Recruitment of p65, c-Rel and IκBβ to the TNF-α promoter was also confirmed in wild-type bone-marrow-derived macrophages (BMDMs; Fig. 3e). In the $I\kappa B\beta^{-/-}$ BMDM, both p65 and c-Rel are recruited normally to the TNF-α promoter. However, when we performed immunoprecipitation with anti-p65, c-Rel and IκBβ are pulled down in wild-type but not $I\kappa B\beta^{-/-}$ BMDMs (Fig. 3f). Therefore, p65 and c-Rel fail to form a stable complex in $I\kappa B\beta^{-/-}$ cells. Thus, the p65 and c-Rel recruited to the TNF-α promoter in $I\kappa B\beta^{-/-}$ cells are not a p65:c-Rel complex. These data suggest that optimal TNF-α transcription requires a ternary complex of IκBβ:p65:c-Rel binding to the TNF-α promoter.

To identify the κB site for p65:c-Rel binding we performed EMSAs using the three κB sites from the TNF-α promoter as probes (κB2, κB2a and κB3; Supplementary Fig. 6b). We identified two distinct

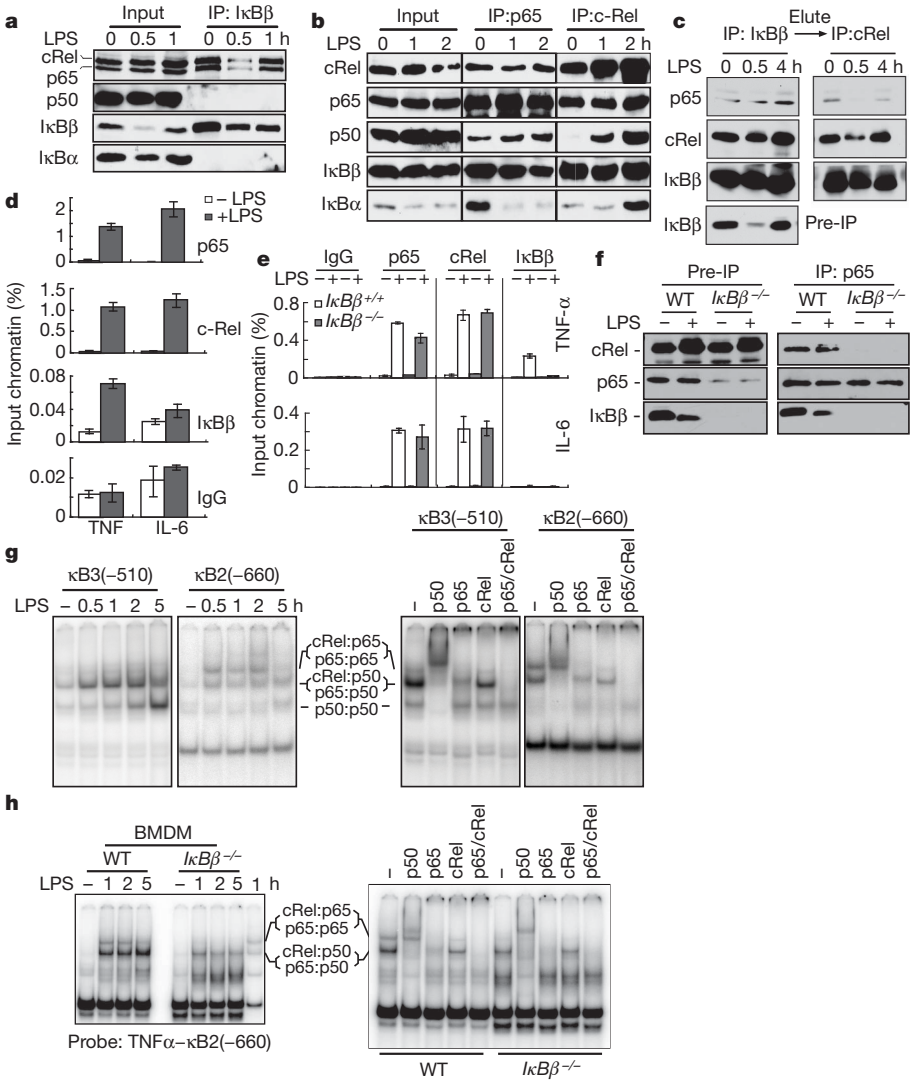

Figure 3 | IκBβ is recruited to the promoter of TNF-α with p65 and c-Rel. **a**, **b**, Raw264.7 were stimulated with LPS and immunoprecipitated (IP) with anti-IκBβ (**a**), anti-p65 (**b**) or anti-c-Rel (**b**) antibodies and immunoblotted as indicated. **c**, LPS-stimulated Raw264.7 lysates were immunoprecipitated with anti-IκBβ, eluted with IκBβ peptide, immunoprecipitated with anti-c-Rel antibody and immunoblotted as indicated. **d**, Raw264.7 lysates were subjected to chromatin immunoprecipitation as indicated and analysed by qPCR targeting TNF-α and IL-6 promoter κB sites; error bars, s.d. ($n = 3$). **e**, Chromatin immunoprecipitation was performed as in **d** on wild-type and $I\kappa B\beta^{-/-}$ BMDMs treated with LPS for 2 h; error bars, s.d. ($n = 3$). **f**, BMDMs treated as in **e** were immunoprecipitated with anti-p65 antibody. **g**, RAW264.7 were treated with LPS and nuclear extracts were subjected to EMSA with TNF-α κB3 or κB2 probes. Super shifts were performed using cells stimulated for 1 h. **h**, BMDMs were treated with LPS and EMSA and supershifts with the κB2 probe were performed as in **g**.

gel-shift patterns. κB3 and κB2a show two major bands (only κB3 is shown in Fig. 3g) whereas κB2 shows three major inducible shift bands. The components of the bands were identified by super-shift assay (Fig. 3g, right panel). The top band in the κB2 gel-shift is mostly p65:c-Rel. Interestingly, the κB2 site possesses features predicted to favour p65:c-Rel binding (Supplementary Fig. 6c). Similar κB binding sites in the CD40 and CXCL1 promoters also demonstrated coordinate recruitment of IκBβ, p65 and c-Rel (Supplementary Fig. 6d). Furthermore, deletion of the κB2 site from a TNF-α promoter reporter abrogated IκBβ-dependent reporter gene expression (Supplementary Fig. 7). In $I\kappa B\beta^{-/-}$ BMDMs, the p65:c-Rel complex binding to the κB2 in EMSA assays is missing (Fig. 3h), in agreement with the immunoprecipitation result. Therefore optimal TNF-α transcription requires a p65:c-Rel complex, stabilized by hypophosphorylated IκBβ, binding to the κB2 site in the TNF-α promoter.

To identify other genes affected by IκBβ deficiency, we examined gene expression profiles in wild-type and $I\kappa B\beta^{-/-}$ BMDMs (Fig. 4a). As expected, *TNF-α* and *IκBβ* are among the genes whose expression is affected by IκBβ deficiency whereas IL-6 and IL-1β are not affected (Fig. 4b). Of the genes whose expression is reduced in the $I\kappa B\beta^{-/-}$ cells, we identified 14 with expression patterns resembling TNF-α (Fig. 4b). The expression of these genes was also reduced in p65, c-Rel or p65/c-Rel knockout fetal liver macrophages, which suggests that LPS-induced expression of these genes might depend on a mechanism similar to TNF-α (data not shown). The expression of TNF-α, IL-1α, IL-6 and IL-1β in response to LPS was further examined by RNase protection (Fig. 4c) and reverse transcription with quantitative real-time PCR (qRT–PCR) (Supplementary Fig. 8), which demonstrated that the reduction in persistent expression of TNF-α in $I\kappa B\beta^{-/-}$ cells is unique. Reduced *IL12b* mRNA and protein secretion in the knockout TEPMs was confirmed by qRT–PCR (Fig. 4d) and ELISA (Fig. 4e). Notably, transcription of *IL12b*, which has a κB site similar to κB2 of TNF-α (Supplementary Fig. 6c), has previously been shown to require c-Rel and be partly dependent on p65 (ref. 26). Thus, only a select group of NF-κB-dependent genes are diminished similarly to TNF-α upon IκBβ deletion. As TNF-α plays a key role in inflammation, we wanted to test whether $I\kappa B\beta^{-/-}$ deletion would affect the course of inflammatory diseases.

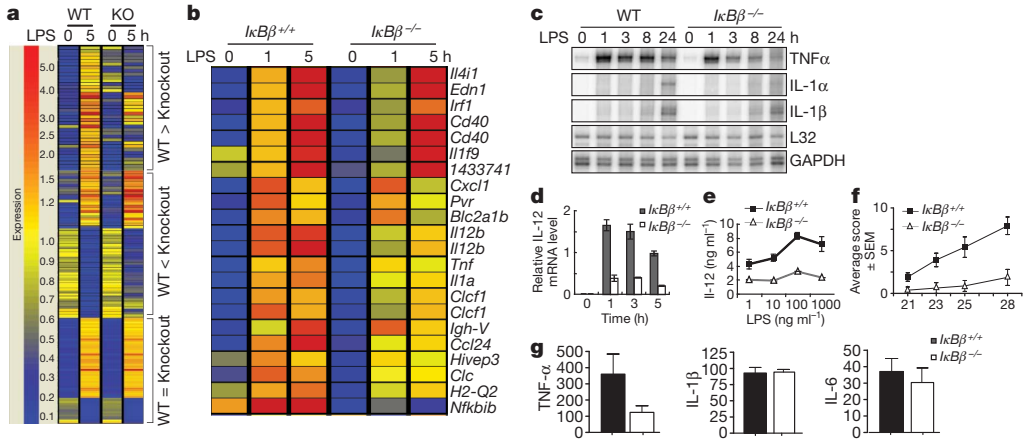

Figure 4 | IκBβ knockout selectively affects only certain LPS-responsive genes and attenuates collagen-induced arthritis. a, LPS-responsive genes whose expression is either downregulated, upregulated or unchanged in $I\kappa B\beta^{-/-}$ BMDMs. **b**, Host–pathogen interaction genes that are IκBβ dependent, LPS-responsive and whose expression pattern resembles TNF-α. **c**, RNase protection assay using wild-type and $I\kappa B\beta^{-/-}$ MEF stimulated with LPS. **d**, IL-12b relative mRNA level in TEMP determined by qRT–PCR; error bars, s.d. ($n = 3$). **e**, ELISA for IL-12p40 secreted from wild-type and $I\kappa B\beta^{-/-}$ TEPMs stimulated with LPS for 20 h; error bars, s.d. **f**, Arthritis clinical scoring in wild-type ($n = 10$) or $I\kappa B\beta^{-/-}$ ($n = 8$) DBA/1J mice; error bars, s.e.m. **g**, Serum TNF-α, IL-1β and IL-6 levels in wild-type or $I\kappa B\beta^{-/-}$ DBA/1J mice in **f**; error bars, s.e.m.

Rheumatoid arthritis is a common inflammatory disease with morbidity resulting from ongoing release of pro-inflammatory cytokines, including TNF-α, and consequent destruction of joint tissue[27]. Previous studies have shown that NF-κB plays a key role in mouse models of arthritis and that blocking NF-κB has a dramatic effect in preventing disease[28,29]. Rheumatoid arthritis can also be effectively treated by anti-TNF-α therapies, although there are significant side-effects[30]. The ability to block only persistent TNF-α expression would be therapeutic without blocking beneficial TNF-α responses, including the expression of innate immune response genes. We therefore tested whether the lack of IκBβ altered the course of collagen-induced arthritis, a well-characterized mouse model of rheumatoid arthritis.

To induce collagen-induced arthritis, we immunized DBA/1J mice with bovine type II collagen. $I\kappa B\beta^{-/-}$ mice displayed delayed onset, lower incidence and decreased severity of collagen-induced arthritis (Fig. 4f and Supplementary Fig. 9). Inflammation in the wild-type mice extended from the paws and digits to the ankle joints and distally through the limb (data not shown). In contrast, $I\kappa B\beta^{-/-}$ mice showed minimal visual signs of paw and joint swelling (Supplementary Fig. 9c). Serum TNF-α was markedly decreased in $I\kappa B\beta^{-/-}$ mice whereas other pro-inflammatory cytokines were not significantly affected (Fig. 4g and Supplementary Fig. 10). Therefore the absence of IκBβ limits the progression and severity of arthritis by reducing the chronic production of TNF-α.

The results presented above demonstrate a dual role for IκBβ: during the early stages of LPS stimulation, NF-κB complexes released by IκBβ degradation contribute to the initial expression of TNF-α (Supplementary Fig. 1). Then, newly synthesized hypophosphorylated IκBβ facilitates the formation of IκBβ:p65:c-Rel complexes, which selectively bind to the κB2 site in the TNF-α promoter, augmenting transcription. As shown in the gene chip and RNase protection assays, this is a relatively selective function and $I\kappa B\beta^{-/-}$ mice are, therefore, otherwise normal. Hence targeting IκBβ might be a promising new strategy to treat chronic inflammatory diseases such as arthritis.

METHODS SUMMARY

Mice. IκBβ-deficient mice were generated by standard homologous recombination in the CJ7 ES cell line using a targeting construct that replaced exons 2 to 5 with a G418-resistance gene. Screened ES cell clones were injected into blastocysts derived from C57BL/6 mice to give rise to $I\kappa B\beta^{-/+}/I\kappa B\beta^{+/+}$ chimaeras. Germline transmission of the disrupted allele was obtained and verified by Southern blotting and PCR, and mice were backcrossed at least ten generations onto the C57BL/6 background. Mice were backcrossed at least eight generations onto the DBA background for collagen-induced arthritis experiments. Mice were maintained in pathogen-free animal facilities at Yale Medical School.

Cells. Wild-type and *IκBβ* knockout MEFs were generated from embryos at embryonic day 12.5 after timed breeding of $I\kappa B\beta^{+/-}$ animals. TEPMs were obtained from 6- to 8-week-old littermate mice 3 days after intraperitoneal injection with thioglycollate. BMDMs were collected by standard protocols and differentiated with 30% L929 supernatant-conditioned media.

Biochemistry. Cell fractionation, western blotting, EMSA, and immunoprecipitations were performed as previously described unless otherwise indicated[6].

LPS-induced shock. LPS-induced shock was tested by intraperitoneal injection of 50 μg g^{-1} body weight LPS and monitoring for survival. In a separate identical experiment, the mice were bled at 1 h and 2 h after LPS treatment and the concentrations of TNF-α, IL-6 and IL-1β in the serum were measured by ELISA.

Intracellular cytokine analysis. Pro-TNF-α levels were analysed in TEPMs after LPS stimulation and brefeldin-A treatment. TNF-α was detected after cell permeabilization by using standard intracellular cytokine staining and flow cytometry.

qRT–PCR. RNA expression was quantified by two-step SYBR qRT–PCR, and relative mRNA levels were obtained by normalizing the readout for each specific gene by that of β-actin.

Microarray analysis. Microarrays for gene expression analyses were performed on BMDMs stimulated with LPS and Affymetrix Mouse Genome 430A 2.0 arrays as per the manufacturer's protocol.

Full Methods and any associated references are available in the online version of the paper at www.nature.com/nature.

Received 5 August 2009; accepted 11 June 2010.

1. Hayden, M. S. & Ghosh, S. Shared principles in NF-κB signaling. *Cell* **132**, 344–362 (2008).
2. Malek, S., Chen, Y., Huxford, T. & Ghosh, G. IκBβ, but not IκBα, functions as a classical cytoplasmic inhibitor of NF-κB dimers by masking both NF-κB nuclear localization sequences in resting cells. *J. Biol. Chem.* **276**, 45225–45235 (2001).
3. Tergaonkar, V., Correa, R. G., Ikawa, M. & Verma, I. M. Distinct roles of IκB proteins in regulating constitutive NF-κB activity. *Nature Cell Biol.* **7**, 921–923 (2005).
4. Hoffmann, A., Levchenko, A., Scott, M. L. & Baltimore, D. The IκB-NF-κB signaling module: temporal control and selective gene activation. *Science* **298**, 1241–1245 (2002).
5. Cheng, J. D. *et al.* Functional redundancy of the nuclear factor κB inhibitors IκBα and IκBβ. *J. Exp. Med.* **188**, 1055–1062 (1998).
6. Thompson, J. E. *et al.* IκB-β regulates the persistent response in a biphasic activation of NF-κB. *Cell* **80**, 573–582 (1995).
7. Weil, R., Laurent-Winter, C. & Israel, A. Regulation of IκBβ degradation. Similarities to and differences from IκBα. *J. Biol. Chem.* **272**, 9942–9949 (1997).
8. Kerr, L. D. *et al.* The rel-associated pp40 protein prevents DNA binding of Rel and NF-κB: relationship with IκBβ and regulation by phosphorylation. *Genes Dev.* **5**, 1464–1476 (1991).

9. Tran, K., Merika, M. & Thanos, D. Distinct functional properties of IκBα and IκBβ. *Mol. Cell. Biol.* **17,** 5386–5399 (1997).
10. Suyang, H., Phillips, R., Douglas, I. & Ghosh, S. Role of unphosphorylated, newly synthesized IκBβ in persistent activation of NF-κB. *Mol. Cell. Biol.* **16,** 5444–5449 (1996).
11. Phillips, R. J. & Ghosh, S. Regulation of IκBβ in WEHI 231 mature B cells. *Mol. Cell. Biol.* **17,** 4390–4396 (1997).
12. Malek, S. *et al.* X-ray crystal structure of an IκBβ•NF-κB p65 homodimer complex. *J. Biol. Chem.* **278,** 23094–23100 (2003).
13. Ernst, M. K., Dunn, L. L. & Rice, N. R. The PEST-like sequence of IκBα is responsible for inhibition of DNA binding but not for cytoplasmic retention of c-Rel or RelA homodimers. *Mol. Cell. Biol.* **15,** 872–882 (1995).
14. Memet, S. *et al.* IκBε-deficient mice: reduction of one T cell precursor subspecies and enhanced Ig isotype switching and cytokine synthesis. *J. Immunol.* **163,** 5994–6005 (1999).
15. Hertlein, E. *et al.* RelA/p65 regulation of IκBβ. *Mol. Cell. Biol.* **25,** 4956–4968 (2005).
16. Klement, J. F. *et al.* IκBα deficiency results in a sustained NF-κB response and severe widespread dermatitis in mice. *Mol. Cell. Biol.* **16,** 2341–2349 (1996).
17. Beg, A. A., Sha, W. C., Bronson, R. T. & Baltimore, D. Constitutive NF-κB activation, enhanced granulopoiesis, and neonatal lethality in IκBα-deficient mice. *Genes Dev.* **9,** 2736–2746 (1995).
18. Goudeau, B. *et al.* IκBα/IκBε deficiency reveals that a critical NF-κB dosage is required for lymphocyte survival. *Proc. Natl Acad. Sci. USA* **100,** 15800–15805 (2003).
19. Hayden, M. S., West, A. P. & Ghosh, S. NF-κB and the immune response. *Oncogene* **25,** 6758–6780 (2006).
20. Rittirsch, D., Flierl, M. A. & Ward, P. A. Harmful molecular mechanisms in sepsis. *Nature Rev. Immunol.* **8,** 776–787 (2008).
21. Evans, G. F., Snyder, Y. M., Butler, L. D. & Zuckerman, S. H. Differential expression of interleukin-1 and tumor necrosis factor in murine septic shock models. *Circ. Shock* **29,** 279–290 (1989).
22. Kontoyiannis, D. *et al.* Impaired on/off regulation of TNF biosynthesis in mice lacking TNF AU-rich elements: implications for joint and gut-associated immunopathologies. *Immunity* **10,** 387–398 (1999).
23. Han, J., Brown, T. & Beutler, B. Endotoxin-responsive sequences control cachectin/tumor necrosis factor biosynthesis at the translational level. *J. Exp. Med.* **171,** 465–475 (1990).
24. Chu, Z. L. *et al.* Basal phosphorylation of the PEST domain in the IκBβ regulates its functional interaction with the c-*rel* proto-oncogene product. *Mol. Cell. Biol.* **16,** 5974–5984 (1996).
25. Kuprash, D. V. *et al.* Similarities and differences between human and murine TNF promoters in their response to lipopolysaccharide. *J. Immunol.* **162,** 4045–4052 (1999).
26. Sanjabi, S. *et al.* Selective requirement for c-Rel during IL-12 P40 gene induction in macrophages. *Proc. Natl Acad. Sci. USA* **97,** 12705–12710 (2000).
27. Brennan, F. M. & McInnes, I. B. Evidence that cytokines play a role in rheumatoid arthritis. *J. Clin. Invest.* **118,** 3537–3545 (2008).
28. Miagkov, A. V. *et al.* NF-κB activation provides the potential link between inflammation and hyperplasia in the arthritic joint. *Proc. Natl Acad. Sci. USA* **95,** 13859–13864 (1998).
29. Jimi, E. *et al.* Selective inhibition of NF-κB blocks osteoclastogenesis and prevents inflammatory bone destruction *in vivo*. *Nature Med.* **10,** 617–624 (2004).
30. Feldmann, M. Development of anti-TNF therapy for rheumatoid arthritis. *Nature Rev. Immunol.* **2,** 364–371 (2002).

Supplementary Information is linked to the online version of the paper at www.nature.com/nature.

Acknowledgements We thank A. Lin at the Yale W.M. Keck Biostatistics Resource for analysis of microarray data. S.G. was supported by grants from the National Institutes of Health (R37-AI03343).

Author Contributions P.R. characterized the mice and performed most of the experiments, M.S.H. performed the immunoprecipitation experiments and helped in writing the paper, M.L. performed collagen-induced arthritis experiments, D.Z. and A.P.W. performed generation of BMDM cells, A.O. performed some experiments, M.L.S. and D.B. generated the knockout mice, C.L. and A.H. performed the RNAse protection assays, and S.G. conceived the study and wrote the paper.

Author Information The microarray data are deposited in National Center for Biotechnology Information Gene Expression Omnibus under accession number GSE22223. Reprints and permissions information is available at www.nature.com/reprints. The authors declare no competing financial interests. Readers are welcome to comment on the online version of this article at www.nature.com/nature. Correspondence and requests for materials should be addressed to S.G. (sg2715@columbia.edu).

METHODS

Mice. The IκBβ targeting construct contained the G418-resistance gene with recombination arm sequences derived from the genomic sequences flanking IκBβ exons 2 and 5 (Supplementary Fig. 2a). Homologous recombination between the targeting construct electroporated into the 129/SV mouse-derived ES cell line CJ7 and the endogenous IκBβ gene replaced the IκBβ sequences between exons 2 and 5 with the G418 resistance cassette. Homologous recombination was confirmed by hybridizing Southern blots of XbaI-digested ES DNA with probe, indicated in Supplementary Fig. 2a. Injection of mutant ES cell clones carrying the disrupted IκBβ gene into blastocysts derived from C57BL/6 mice gave rise to $I\kappa B\beta^{-/+}$/ $I\kappa B\beta^{+/+}$ chimaeras. Germline-transmittable $I\kappa B\beta^{-/+}$ mice were obtained by crossing chimaeras with C57BL/6 mice. $I\kappa B\beta^{-/+}$ mice (129SvEv background) were then backcrossed at least ten generations onto the C57BL/6 background before experiments. Mice used in the experiments were 6 to 8 weeks old derived by either brother–sister mating of $I\kappa B\beta^{-/-}$ or $I\kappa B\beta^{+/+}$ littermates (for age- and sex-matched mice experiments) or $I\kappa B\beta^{+/-}$ littermates (for littermate experiments). Backcrossed knockout and wild-type mice were maintained in pathogen-free animal facilities at Yale Medical School.

Generation of MEFs. Embryos at embryonic day 12.5 from timed breeding of $I\kappa B\beta^{-/+}$ female and male mice were dissected free of maternal tissues and Reichert's membrane, washed with PBS, sliced into small pieces and shaked with 0.05% trypsin-EDTA (GIBCO) for 30 min at 37 °C. The cells were suspended in DMEM supplemented with 10% fetal bovine serum and plated in 100 mm plates. Wild-type and $I\kappa B\beta^{-/-}$ MEFs were identified by immunoblotting with IκBβ antibody and PCR genotyping using MEF cells.

Antibodies and reagents. Antibodies used were anti-c-Rel, anti-RelB, anti-p52/p100, anti-p50/p105, anti- IκBα, anti-IκBβ, anti-IκBε (Santa Cruz), anti-GAPDH (Research Diagnostics), anti-p65 (BioMol), FITC-conjugated anti-TNF-α (eBiosciences), phycoerythrin-conjugated anti-CD11b and APC-conjugated anti-F4/80 (BD Biosciences). *Escherichia coli* LPS was purchased from Sigma-Aldrich (serotype 055:B5). In some experiments LPS from *Salmonella typhimurium* (Sigma-Aldrich) was used. Recombinant hTNF-α and mIL-1β used in MEF stimulation were from R & D Systems.

Cell fractionation. Cells were incubated in hypotonic buffer (10 mM HEPES pH 7.9, 10 mM KCl, 0.1 mM EDTA, 1 mM DTT, 0.5 mM PMSF, 1 μg ml^{-1} leupeptin) at 4 °C for 15 min. Nonidet-40 was added to a final concentration of 0.05% and lysates were vortexed and centrifuged 1,000*g* for 5 min. Supernatants, containing the cytosolic fraction, were cleared by centrifugation at 20,000*g* for 10 min and were frozen at −80 °C. Nuclear pellets were washed with hypotonic lysis buffer and nuclear protein extracts for EMSA and nuclear immunoprecipitation were prepared by incubating the nuclei in hypertonic buffer (20 mM HEPES pH 7.9, 0.4 M NaCl, 1 mM EDTA, 1 mM DTT, 1 mM PMSF, 1 μg ml^{-1} leupeptin) for 30 min with constant agitation at 4 °C. Nuclear lysates were then isolated after a 10 min spin at 13,000 rpm and frozen at −80 °C.

Western blot. Thirty to fifty micrograms of total protein were run on 12% SDS–polyacrylamide gel electrophoresis gel. After transfer to polyvinylidene fluoride membrane (Millipore), immunoblotting was performed as per the manufacturer's protocol.

EMSA assay. Five micrograms of protein from the nuclear fractions were incubated with ^{32}P-labelled double-stranded NF-κB or NF-Y probe (NF-κB: AGTTGAGGGGACTT TCCCAGG; NF-Y: ACTTTTAACCAATCAGAAAAAT) in binding buffer (5 mM Tris pH 7.5, 25 mM NaCl, 0.5 mM EDTA, 2.5% glycerol, 0.5 mM DTT, PolydI/dC 0.1 μg μl^{-1}, dGTP 3 mM, BSA 0.5 mg ml^{-1}) at room temperature for 15 min and run on a 6% non-denaturing polyacrylamide gel electrophoresis gel in 0.4 × TBE (36 mM Tris, 36 mM boric acid, 0.8 mM EDTA) buffer. Gel was visualized using Storage Phosphor Screen (Amersham Biosciences).

Luciferase assay. MEF cells (2.5×10^5) grown on 12-well plates were transiently transfected using FuGene 6 with the NF-κB-dependent reporter construct pBIIx-luc and the *Renilla* luciferase vector (Promega). Twenty-four hours after transfection, cells were stimulated with LPS (1 μg ml^{-1}), IL-1β (10 ng ml^{-1}) or TNF-α (10 ng ml^{-1}) for 4 h. Unstimulated and stimulated cells were then lysed and luciferase activity was measured using the dual luciferase assay kit (Promega).

LPS-induced endotoxin shock. Age matched 8- to 12-week-old $I\kappa B\beta^{-/-}$ and control mice of both sexes were injected intraperitoneally with 50 μg g^{-1} body weight LPS (Sigma 55:011). Survival was examined every 8 h for up to 4 days. In a separate identical experiment, the mice were bled at 1 h and 2 h after LPS treatment and the concentration of TNF-α, IL-6 and IL-1β in the serum was measured by ELISA (BD Biosciences).

Thioglycollate-elicited peritoneal macrophages. Six- to 8-week-old littermate mice were injected intraperitoneally with 2 ml of 3% thioglycollate broth (Sigma). Three days later, the mice were killed and their peritoneal cavities were washed with 10 ml cold PBS (Gibco). Cell pellets were washed once with DMEM supplemented with 10% FBS and cultured at the concentration of 5×10^5 cells per millilitre. Two hours later the dishes were washed with medium to remove non-adherent cells. At least 75% of the remaining adherent cells were macrophages, as analysed by fluorescence-activated cell sorting (Supplementary Fig. 5a). Cells were cultured overnight in DMEM supplemented with only 0.5% FBS. Cells were then stimulated with LPS (1 μg ml^{-1}). TNF-α, IL-6 and IL-12 secreted in the medium were measured by ELISA. In some experiments cells were lysed and total RNA was prepared for qRT–PCR analysis of relative mRNA level.

Measurement of intracellular pro-TNF-α. Intracellular pro-TNF-α was measured in thioglycollate-elicited peritoneal macrophage stimulated with 1 μg ml^{-1} LPS for 2–8 h. To inhibit pro-TNF-α transportation to the plasma membrane and subsequent cleavage and release of secretive TNF-α, cells were treated with brefeldin A (eBioscience) while being stimulated by LPS. Cells were then scraped off the cell culture plates, washed in PBS and fixed with 1% formaldehyde. After being washed twice in PBS supplemented with 5% calf serum, cells were permeabilized by resuspending in BD Perm/Wash Buffer (BD Biosciences). Intracellular TNF-α was stained by incubating the permeabilized cells with FITC-anti-TNF-α antibody (eBiosciences) diluted in BD Perm/Wash Buffer for 30 min on ice. In some experiments, PE-anti-CD11b and APC-anti-F4/80 antibodies were incubated with TNF-α antibody. After washing with the Perm/Wash Buffer, stained cells were identified by flow cytometry.

BMDM cultures. Macrophages were derived from bone marrow following a standard protocol. Briefly, bone marrow cells were plated overnight to remove stromal cells and mature resident macrophages. Non-adherent cells were transferred to new plates and differentiated with 30% L929 supernatant-conditioned media over 7 days. Macrophages (7×10^5 cells per millilitre) were allowed to adhere overnight and stimulated with 1 μg ml^{-1} LPS.

qRT–PCR. RNAs were prepared using RNeasy Kit (Qiagene). RNA expression was quantified by two-step SYBR real-time RT–PCR (Stratagene). Relative mRNA level was obtained by normalizing the readout of a specific gene by that of β-actin. Oligonucleotide sequences used in quantitative PCR are available upon request.

Chromatin immunoprecipitation. RAW264.7 or BMDM cells were cross linked in 1% formaldehyde at room temperature for 7 min and lysed in RIPA buffer (10 mM Tris, pH 7.4, 0.3 M NaCl, 1 mM EDTA, 1% Triton-X 100, 0.1% NaDOC, 0.1% SDS, 1 mM PMSF, 1 μg ml^{-1} aprotinin and 1 μg ml^{-1} pepstatin A). After centrifugation at 1,700*g* for 5 min, the pellet nuclei were sonicated and chromatin immunoprecipitation was performed according to standard Upstate protocol. Immunoprecipitated chromatins were dissolved in 20 μl water and precipitated DNAs for the κB sites in TNF-α and IL-6 promoter were assayed by SYBR green qPCR with the following primers: TNF-α-fr: TGAGTTGATGTACCGC AGTCAAGA; TNF-α-bk: AGAGCAGCTTGAGAGTTGGGAAGT; IL6-fr: CGA TGCTAAACGACGTCACATTGTGCA; IL6-bk: CTCCAGAGCAGAATGAGCTAC AGACAT.

Microarray analysis. BMDMs were stimulated with LPS (1 μg ml^{-1}) and RNA was prepared with Qiagen RNeasy. Complementary DNA preparation and hybridization to Affymetrix Mouse Genome 430A 2.0 Arrays were performed at the Yale W.M. Keck facility.